

A Finite Element-Based Framework for Understanding the Energy Performance
of Concrete Elements Incorporating Phase Change Materials

by

Lavannya Babanrao Hembade

A Thesis Presented in Partial Fulfillment
of the Requirements for the Degree
Master of Science

Approved November 2012 by the
Graduate Supervisory Committee:

Narayanan Neithalath, Co-Chair
Subramaniam Rajan, Co-Chair
Barzin Mobasher

ARIZONA STATE UNIVERSITY

December 2012

ABSTRACT

Dwindling energy resources and associated environmental costs have resulted in a serious need to design and construct energy efficient buildings. One of the strategies to develop energy efficient structural materials is through the incorporation of phase change materials (PCM) in the host matrix. This research work presents details of a finite element-based framework that is used to study the thermal performance of structural precast concrete wall elements with and without a layer of phase change material. The simulation platform developed can be implemented for a wide variety of input parameters. In this study, two different locations in the continental United States, representing different ambient temperature conditions (corresponding to hot, cold and typical days of the year) are studied. Two different types of concrete – normal weight and lightweight, different PCM types, gypsum wallboards with varying PCM percentages and different PCM layer thicknesses are also considered with an aim of understanding the energy flow across the wall member. Effect of changing PCM location and prolonged thermal loading are also studied. The temperature of the inside face of the wall and energy flow through the inside face of the wall, which determines the indoor HVAC energy consumption are used as the defining parameters. An ad-hoc optimization scheme is also implemented where the PCM thickness is fixed but its location and properties are varied. Numerical results show that energy savings are possible with small changes in baseline values, facilitating appropriate material design for desired characteristics.

ACKNOWLEDGEMENTS

I would like to thank and express my sincere gratitude to my advisors and committee chair, Dr. Narayanan Neithalath and Dr. Subramaniam D. Rajan for their continuous support, encouragement and patience. Their mentoring, motivation and guidance through all my research work and course works have been invaluable. I would also like to extend my gratitude to Dr. Barzin Mobasher for being in my thesis committee.

I would like to thank my friends for all their support and motivation throughout the studies and I am very glad to acknowledge all my classmates and colleagues, especially Vikram Dey, Arumugam Deivanayagam, Amie Stockwell, Kirk Vance, Deepak Ravikumar, Vaidehi Jakkali and Meetan Kaur for their intellectual support and assistance. I would also like to express my gratitude to all the CEE and ASU administrative staffs for their kind help and support.

I dedicate this thesis to my mother, Alka Hembade and to all my family and friends.

TABLE OF CONTENTS

	Page
LIST OF TABLES.....	v
LIST OF FIGURES	vi
ABBREVIATIONS.....	ix
NOMENCLATURE	x
CHAPTER	
1.0 INTRODUCTION	1
2.0 FINITE ELEMENT ANALYSIS AND MODEL.....	14
3.0 PRELIMINARY STUDIES.....	22
3.1 Selection of Suitable PCM.....	22
3.2 Comparison between 10cm and 20cm thick walls.....	27
4.0 EFFECT OF VARYING PCM THICKNESS AND AD-HOC OPTIMIZATION	32
4.1 Typical wall geometry and layout	32
4.2 Concrete and PCM properties.....	33
4.3 Ambient temperature data.....	34
4.4 Results from Numerical Analysis.....	38
4.4.1 PCM for Phoenix	38
4.4.2 PCM for Los Angeles	48
4.4.3 Ad-hoc optimization for thermal efficiency	49

CHAPTER	Page
5.0 USE OF MULTIPLE PCMS AND GYPSUM WALLBOARDS EMBEDDED WITH PCM	55
5.1 Weather Data	55
5.2 Materials and Properties	57
5.3 Model Details.....	59
5.4 Numerical Results.....	62
5.4.1 Use of Both PCM A and PCM C Together	62
5.4.2 Comparison between WB and Pure PCM D.....	70
6.0 CONCLUSIONS & FUTURE WORK.....	79
6.1 Conclusions.....	79
6.2 Future Work.....	82
REFERENCES	83
APPENDIX.....	88
WALL DESIGN PROGRAM	88

LIST OF TABLES

	Page
Table 3-1: Material properties used in the analyses.....	24
Table 3-2 – Material Properties	27
Table 3-3: EFTIF data summary for section 3.3.....	29
Table 4-1: Material properties used in the analyses.....	34
Table 4-2: Radiation-related Data.....	36
Table 4-3: EFTIF Summary Table for Phoenix (PCM-A).....	47
Table 4-4: EFTIF Summary Table for Los Angeles (PCM-B).....	48
Table 4-5: Ad-Hoc Optimization for Centrally Placed PCM Model (Phoenix). ..	51
Table 5-1: Radiation-related Data.....	57
Table 5-2 : Material properties used in the analyses.....	58
Table 5-3: Pure PCM D thickness	59
Table 5-4: EFTIF and Energy savings for a Hot Day.....	66
Table 5-5: EFTIF and Energy savings for a Cold Day	67
Table 5-7: EFTIF data summary for section 4.2.....	72

LIST OF FIGURES

	Page
Figure 1-1: Temperature dependent phase change and energy absorption/release by phase change materials [13].....	3
Figure 1-2: Latent heat contribution of microencapsulated paraffin PCM in cement paste [26]	4
Figure 1-3: Classification of PCMs	9
Figure 2-1: Sensible and Latent heat stored in PCM	14
Figure 2-2: Finite element model (1 m high).....	16
Figure 2-3: Computational framework for finite element analysis.....	17
Figure 2-4: EFTIF versus element size.....	19
Figure 2-5: Inside wall temperature versus element size.....	19
Figure 3-1: (a) Typical plain concrete wall, (b) Wall with a centrally placed 1cm PCM layer	23
Figure 3-2: Comparison of temperature variation at the inside face of concrete wall.....	25
Figure 3-3: Comparison of EFTIF of concrete wall	26
Figure 3-4: Ambient air temperature profile for Phoenix, AZ: (a) without radiation effects, (b) with radiation effects	28
Figure 3-5: EFTIF w.r.t. % of PCM in wall.....	30
Figure 3-6: Maximum energy stored in PCM.....	31
Figure 4-1: (a) Typical concrete wall, (b) Wall with a centrally placed PCM layer, and (c) PCM layer placed closer to the inside face.....	33

	Page
Figure 4-2: Ambient air temperature profile [43]: (a) Phoenix, (b) Los Angeles.	35
Figure 4-3: Ambient air temperature profile with radiation effects for: (a) Los Angeles, and (b) Phoenix. IFAT is also shown for both the cases.	37
Figure 4-4: Temperature variation as a function of time at the inside face of the wall for ambient conditions corresponding to Phoenix: (a) NC, (b) LWC. The results shown are for PCM-A.	40
Figure 4-5: Temperature variation through the wall: (a) NC, (b) LWC	41
Figure 4-6: Energy flow through inner face versus PCM thickness:.....	42
Figure 4-7: Energy flow through inner face with respect to time: (a) NC (b) LWC	43
Figure 4-8: Cumulative sensible energy stored in PCM as a function of time: (a) NC, (b) LWC	45
Figure 4-9: Cumulative latent energy stored in PCM as a function of time: (a) NC, (b) LWC	46
Figure 4-10: Temperature at various locations in the wall and energy flow as a function of time for <i>Combination 5-2</i>	53
Figure 4-11: Comparison of: (a) energy flow through the inside face (EFTIF), and (b) inside face temperatures for <i>Combinations 5-1</i> and <i>5-2</i>	54
Figure 5-1: Ambient air temperature profile for Phoenix, AZ [43] (a) without radiation (b) with radiation	56
Figure 5-2: (a) Plain concrete wall (b) Both PCMs placed separately (5 Layer Model).....	60

	Page
Figure 5-3: (a) Plain concrete wall (b) Concrete wall with centrally placed gypsum WB	61
Figure 5-4: Temperature of the inside face for Case AC-5	63
Figure 5-5: Temperature of the inside face for Case CA-5	63
Figure 5-6: Cumulative latent energy stored in (a) PCM A and (b) PCM C for Case AC-5; and in c) PCM A and (d) PCM C for Case CA-5	64
Figure 5-7: EFTIF (a) for Case AC-C; (b) for Case CA-C.....	65
Figure 5-8: Energy flow at different points across wall thickness (a) Case C-3 (b) Case CA-5 (c) Case AC-5.....	68
Figure 5-9: Temperature variation inside the room with respect to time	71
Figure 5-10: (a) Energy flow into and out of the room with respect to thickness (b) Energy flow into and out of the with respect to time	73
Figure 5-11: (a) Sensible energy (b) Latent energy; stored in PCM with respect to time	75
Figure 5-12: Temperature of inside face (b) EFTIF with respect to time over one week	76
Figure 5-13: Net latent energy stored in PCM each day.....	77
Figure 5-14: Latent energy stored in PCM with respect to time over	78
Figure 6-1: WallDesign Program.....	89
Figure 6-2: Procedure to start program.....	90
Figure 6-3: Model details for sample input file	100

ABBREVIATIONS

PCM	Phase Change Material
TES	Thermal Energy Storage
CA	California
AZ	Arizona
NC	Normal Concrete
LWC	Light Weight Concrete
WB	Gypsum Wall Board
HVAC	Heating, Ventilation and Air-Conditioning
EFTIF	Energy Flow Through Inside Face
PCME	PCM Efficiency
FE/FEA	Finite Element / Analysis
PEG	Poly-Ethylene Glycol
PCT	Phase Change Temperature
LHC	Latent Heat Capacity
SHC	Sensible Heat Capacity
IFAT	Inside Face Air Temperature

NOMENCLATURE

ρ	Density (kg/m ³)
C_p	Specific heat capacity (J/kg-C)
k	Thermal conductivity (W/m-C)
ΔH	Latent heat capacity (J/kg)
T	Temperature (C)
T_m	Phase change temperature (C)
t	Time (s)
α	Solar coefficient of absorption
S	Total solar radiation (W/m ²)
h	Convective co-efficient (W/m ² -C)
τ	Heat flux (W/m ²)
A	Area (m ²)
m	Mass (kg)
Q_s	Heat absorbed as sensible energy (J)
Q_L	Heat absorbed as latent energy (J)
Q_T	Total heat absorbed (J)
E	Energy (J)

Subscripts

<i>e</i>	Exterior
<i>int</i>	Interior
<i>i</i>	Initial
<i>f</i>	Final
<i>eq</i>	Equivalent

1.0 INTRODUCTION

One of the greatest engineering challenges of the 21st century relates to energy sustainability. Buildings consume more than a third of the world's energy, and the use is expected to grow as the population increases or becomes more urban and affluent. In the United States, the building sector accounts for about 40% of the primary energy use, compared to 32% for the industrial sector and 28% for the transportation sector [1]. The use of electric power and heat in buildings contribute to about 40% of the US greenhouse gas emissions [1]. Based on the current trends, it is anticipated that buildings will become the majority energy consumers by 2025 and would use as much energy as industry and transportation sectors combined by 2050 [2]. Therefore it is obvious that reducing the energy consumption in buildings can contribute significantly to the reduction of dependence on foreign sources of energy, and reduction in greenhouse gas emission.

Phase Change Materials:

PCMs have high heats of fusion which help provide more energy savings over all other energy storage materials. Heat is stored in a PCM is either sensible heat or latent heat. Sensible heat storage occurs when the heat transferred to any storage medium leads to a temperature increase in the medium. Latent heat storage occurs during phase transition of a material without increasing the temperature of the medium. PCMs compose of a huge range of material classes - organic, inorganic or eutectic mixes of both which have been explained in detail

later. The difference between using a common insulator and a PCM is due to the additional latent heat storage capacity of a PCM. Higher the melting enthalpy, more is the energy storage and lesser is the heat flow across the PCM layer. Also, a lower thermal conductivity leads to lesser heat flow across the PCM layer. Numerous analyses have been run for the opted locations with different PCMs and the most favorable for each location were chosen.

Considerable energy savings in the built environment can be realized if the heating and cooling loads in buildings can be controlled. One potential passive methodology to attain this objective is through the use of thermal energy storage (TES) materials. TES can either be accomplished using sensible heat storage or latent heat storage [3, 4, 5]. While sensible heat storage systems rely on the specific heat capacity and density (or mass) of the material to store heat, they suffer from disadvantages related to low storage capacity per unit volume and non-isothermal behavior during heat storage and release [5, 6, 7]. This has led to substantial interest in the use of Phase Change Materials (PCM), which are latent heat storage materials, in building applications [8, 9, 10, 11, 12]. PCMs store energy when subjected to temperatures in excess of their melting point by changing from the solid to the liquid state. The stored energy is released when the temperature drops below the melting point of the PCM. A schematic of this process is depicted in Figure 1-1[13]. It is primarily the latent heat contribution that drastically increases the energy storage capacity of PCMs when compared to sensible heat storage media, depending on the nature of the PCM and the temperature range of interest [5,14]. In building energy conservation applications,

PCM can serve twin purposes: (i) it can store the solar energy and release it when the indoor temperatures fall, and (ii) it can be used to shift the building heating or cooling load from peak to off-peak electricity periods [15, 16, 17, 18].

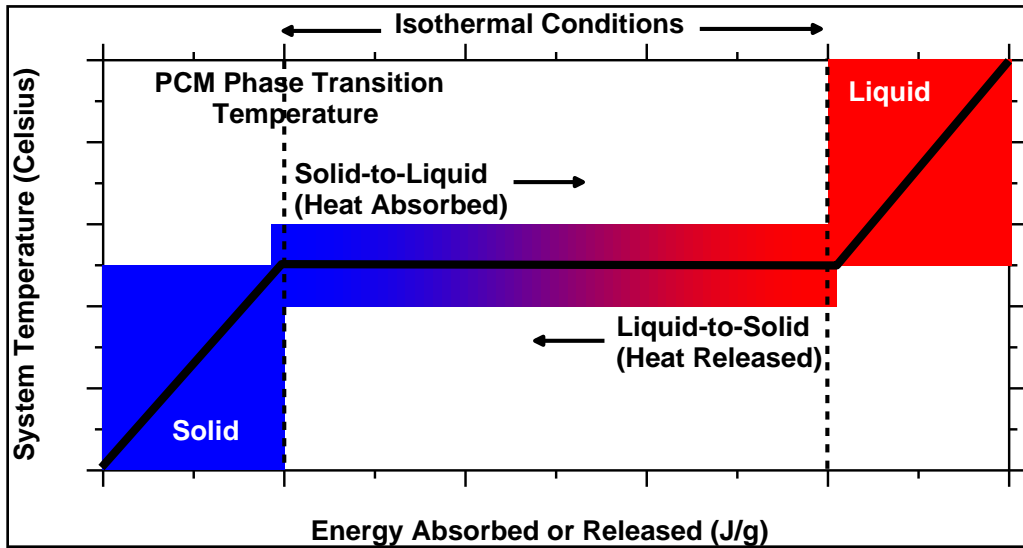


Figure 1-1: Temperature dependent phase change and energy absorption/release by phase change materials [13].

A number of recent studies have investigated the use of different types of PCMs as integral component of building elements such as wallboards, concretes, and plastering mortars for TES applications [8, 19, 20, 21]. The method of incorporation of PCMs, by impregnation into the porous building material such as wallboard or concrete, or micro- and macro-encapsulation, have also been adequately addressed in the literature [20, 22, 23, 24, 25]. Figure 1-2 shows the relationship between heat energy absorbed by a cement paste when 5% of a microencapsulated PCM by mass is incorporated as an integral component of the paste [26]. In the phase transition temperature range (between 22°C – 24°C in this

case), the energy absorption capacity of the cement paste is enhanced by more than three times because of the incorporation of the PCM.

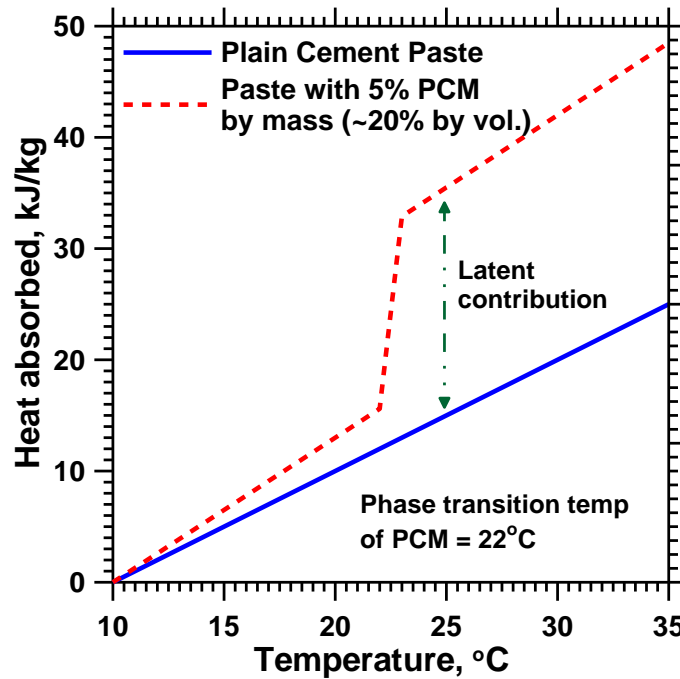


Figure 1-2: Latent heat contribution of microencapsulated paraffin PCM in cement paste [26]

The energy performance of prototype structures made using PCM-integrated components has also been reported [26,27,28,29]. Numerical analyses of energy performance of buildings enclosed by PCM incorporated elements have also been reported in several studies. Many of these studies have carried out simulations in order to determine the optimal orientation of walls containing PCMs, parameters relating to the thermal inertia of system such as wall thickness, thermal conductivity, and heat capacity, and variation of internal temperature in enclosures subjected to passive cooling or without any climatic control [8, 24, 30, 31]. While a number of studies have examined the energy efficiency of elements containing phase change materials, the boundary conditions relating to the

external temperature are such that the maximum difference between the desired indoor temperature and the maximum external temperature is not more than 10-15°C, even including the effects of radiation [23, 32, 33]. The conclusions arrived at based on optimization studies under these conditions (for e.g., the optimal PCM layer thickness, maximum latent energy storage capacity) might not be directly applicable when the ambient and desired temperature differences are extremely high (in the range of 25°C, as in desert summers). This aspect is also considered in this study.

Gypsum Wallboards

One of the most effective methods of incorporating PCMs into building components is embedding PCMs into gypsum wall boards either by immersion of wallboards into a PCM bath or by direct mixing of PCM with gypsum prior to manufacture of the wall boards. However, due to interaction of PCM with the wallboard elements, leakage of liquid PCMs etc. the immersion method is the most popular method of PCM incorporation. Gypsum wallboards with higher porosity are more feasible for immersion. Percentage of PCM absorbed by a wallboard of course depends on time of immersion, temperature of bath, compatibility between wallboard and PCM. Higher amount of PCM is absorbed for higher immersion times [34, 35, 36], though increasing amount of PCM in the wallboards constitutes to increased fire-hazard risks. [34, 35] tested two methods of eliminating fire-hazards – limiting the amount of imbibed PCM to 20% or further treating the wall board with an insoluble fire retardant. Several studies and experiments have been conducted on PCM treated wallboards to find their

physical, chemical and thermal properties [37, 38, 39]. Studies on a range of PCMs have also shown certain types of PCMs to be better suited for incorporation into gypsum wallboards like – Coconut fatty acids [37], Capric and Lauric acids [38], Paraffins [34, 35, 36]. Use of PCM treated wallboards over conventional wallboards increases thermal efficiency of buildings to a large extent and maybe the easiest method of PCM incorporation. Incorporating wallboards into a wall is most feasible and economic. Full scale experiments on rooms have shown that incorporation of PCM wallboards in walls reduce air temperature fluctuations in the room [24, 40].

Multiple PCMs

The use of multiple PCMs has become a popular method for thermal energy storage in the recent years because of their potential for enhanced thermal performance. (Gong and Mujumdar, 1996) [41] developed a finite element model to study alternate melting and freezing heat transfer through several combinations of PCMs. They discovered that charge-discharge rates of thermal energy can be significantly enhanced using various PCMs depending on arrangement of the PCMs, thermo physical properties and applied boundary conditions. (Shaikh and Lafdi, 2006) [42] developed a heat storage system using multiple rectangular slabs with different PCMs considering combined convection and diffusion. They studied the effect of buoyancy induced motion in the propagation of the melt interface of different PCM layers placed in series or parallel configuration. They concluded that for the same set of thermophysical properties, the total energy storage of the composite PCM arrangement can be enhanced much more than that

of a single PCM slab, by using PCMs with different phase change temperatures. Diaconu and Cruceru [18] developed a new composite wall system (three layer sandwich type insulating panel) with outer layers of PCM wallboards. Both PCM layers have different thermal functions- the outer layer has a higher melting point and is active only during the hot season whereas the inner layer has a lower melting point and is active in a cooler season. It is seen that presence of both these layers reduces annual energy demand and reduces peak heating/cooling loads. The current research work branches out on the above results to study effect of inter-changing PCM location with respect to the other and placing both PCMs at different points in the wall cross-section, although the study is concentrated for Phoenix, AZ area.

Classification of PCMs

PCMs can be classified into three major categories viz. Eutectic, Organic and Inorganic. Eutectics can be made by combining two organic compounds, two inorganic compounds or an inorganic and an organic compound. Most commonly used are eutectic water-salt solutions which have good storage density and melting temperatures below 0°C due to addition of the salts [4]. Pure salts, inorganic mixtures and salt hydrates are types of inorganic PCMs. Organic PCMs include paraffins, fatty acids, sugar alcohols, polyethylene glycols and calthrates. Examples of each type of PCM can be seen from Figure 1-3: Classification of PCMs. Advantages and disadvantages of organic PCMs are listed on the next page.

Advantages

- Safe, non-corrosive, non-toxic, non-reactive
- Chemically and thermally stable
- No or little sub cooling
- Microencapsulation possible
- Show low thermal conductivity
- Self-nucleating (speeds solidification)
- Do not Segregate
- Exhibit ability to melt congruently

(i.e. no change in composition occurs during melting)

Advantages and disadvantages of inorganic PCMs are listed below.

Advantages

- High melting enthalpy
- High density
- Non-flammable
- Low cost
- Easy availability
- High volumetric latent heat storage capacity

Disadvantages

- Low volumetric latent heat storage capacity
- Lower density
- Flammable
- Lower melting enthalpy
- Relatively more expensive
- Show sub cooling effect
- Corrosive
- Cycling stability
- Microencapsulation impossible
- High thermal conductivity
- Nucleating agents required especially after repeated cycling

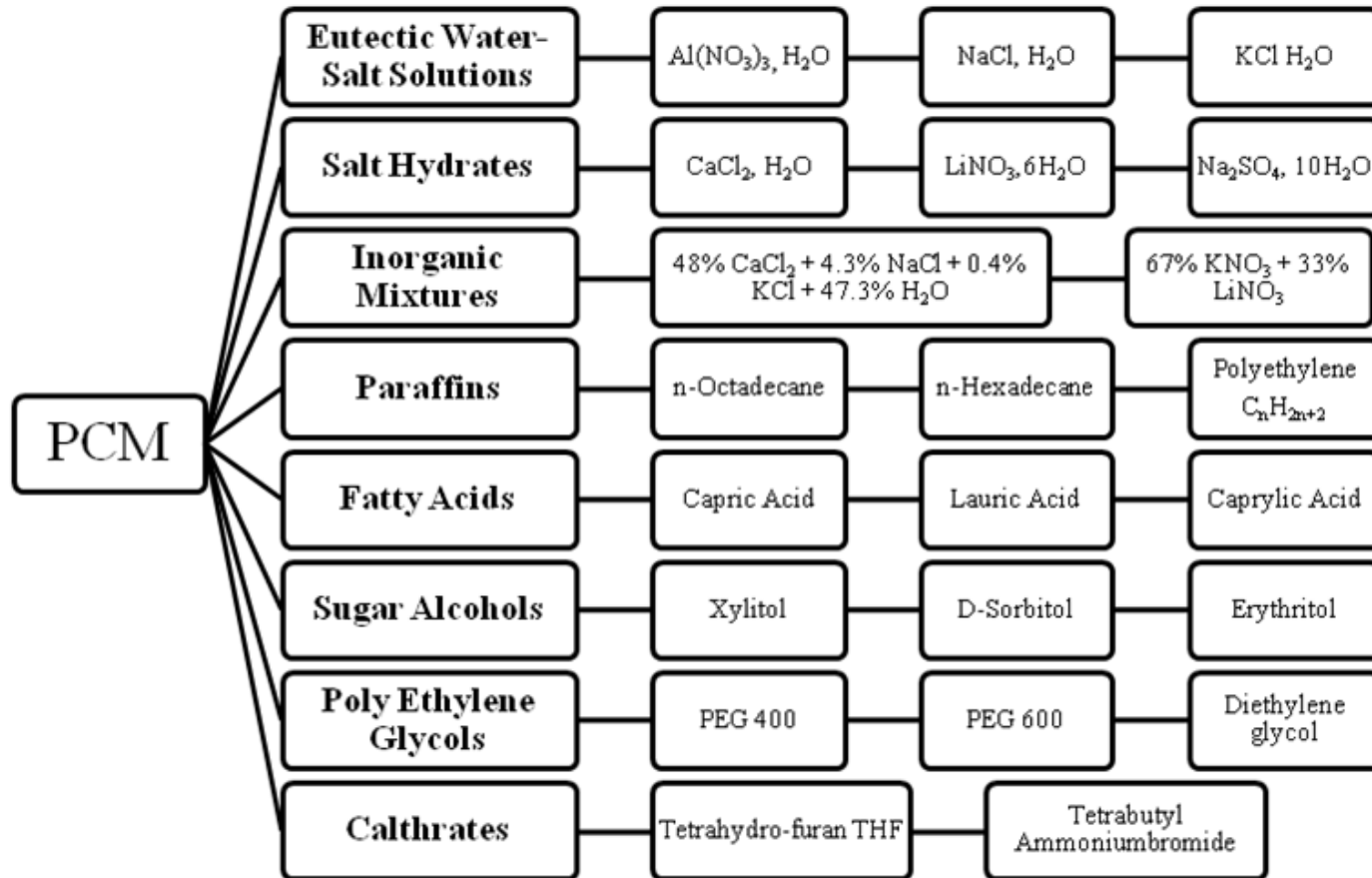


Figure 1-3: Classification of PCMs

Applications of PCM

PCMs have a wide range of applications from transportation to medical and health purposes. Some of the applications have been shown in



Thermal wear including vests, jackets, pants and underwear. Different PCMs are integrated into clothes making them suitable for regulating body temperature of people working in extreme climatic conditions.



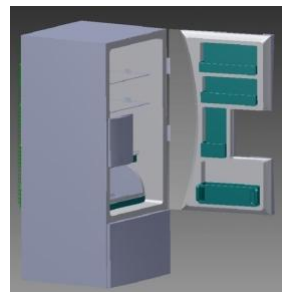
Transportation and storage of food especially perishable items over long distances or in areas like cargo bays of airplanes where there is no access to electricity to use coolers or heaters.



Warmers and sleeping bags. This is just another extension to integrating PCMs in clothes intended solely for the purpose of human comfort.



Medical applications: Storage and transportation of blood, plasma or drugs that need stocking at very specific temperatures.



In heat exchangers like refrigerators, air coolers, heaters. Incorporation of PCMs in these devices shows a significant reduction in energy consumption of the appliances.



PCMs are incorporated into building elements like concrete, precast blocks, tiles, wallboards, plaster etc to help regulate energy utilization by the room heating and cooling systems

Objectives

The present study focuses on providing answers to the following questions.

- (1) How does the use of pure phase change materials embedded as a distinct layer in a typical wall configuration influence the energy flow through the wall?
- (2) Does PCM location within the wall play a role in energy consumption?
- (3) How do external temperatures influence the selection of optimal PCM thickness and material properties?
- (4) How do gypsum wallboards behave when embedded with PCM?
- (5) How does use of multiple PCM layers affect energy consumption as opposed to use of a single PCM layer?

This research work presents a finite element simulation of transient heat transfer through structural precast concrete wall elements with and without a layer of phase change material. Two different PCM types and different PCM layer

thicknesses are considered in order to develop a fundamental understanding of the energy flow across the wall member as a function of the PCM characteristics and its location in the wall. Active temperature control in the enclosure is considered in this study. An ad-hoc optimization scheme is also implemented where the PCM thickness is fixed but its location and properties are varied. It is believed that this framework will lead to optimal selection of PCM parameters for a given set of external and internal temperature profiles. Effect of multiple PCM layers placed together or separately in the same wall has been studied and results discussed. Use of PCM incorporated gypsum board, along with effects of different wall thicknesses have also been discussed here.

Four different temperature profiles (corresponding to two different locations in the continental USA) are considered. First one represents a typical summer day in Los Angeles, CA and the others represent a hot day, a cold day and a typical day in Phoenix, AZ. The baseline wall is made up of normal concrete (NC) or lightweight concrete (LWC), and the thermal performance of the PCM incorporated elements are compared against the baseline walls. Several model parameters are studied and they include: (a) the energy needed to maintain the interior temperature at a specified human comfort level temperature that varies with time of day, (b) the relationship between PCM thickness and the efficiency of the PCM to act as a thermal storage and barrier system, and (c) guidelines for designing the PCM thickness and location in the wall, considering the thermal efficiencies (the structural efficiency also needs to be a part of the discussion, which is covered in an on-going study).

2.0 FINITE ELEMENT ANALYSIS AND MODEL

Heat transfer problems involving conduction, forced convection, and boundary radiation can be analyzed in ABAQUS. Current analysis assumes that the thermal and mechanical properties are independent of each other or uncoupled i.e. time rate of internal energy is independent of strains and displacements of the body and dependent only on the temperature at any given time. ABAQUS defines the relationship between specific heat (c) and the time rate of Internal energy (U) as in Equation (2.1); except for when phase change materials are used (rather phase change is specified).

$$c = \frac{dU}{dT} \quad (2.1)$$

The inclusion of the latent heat and phase change temperatures makes the analysis non-linear. Latent heat is considered in addition to the specific heat (as seen in Figure 2-1).

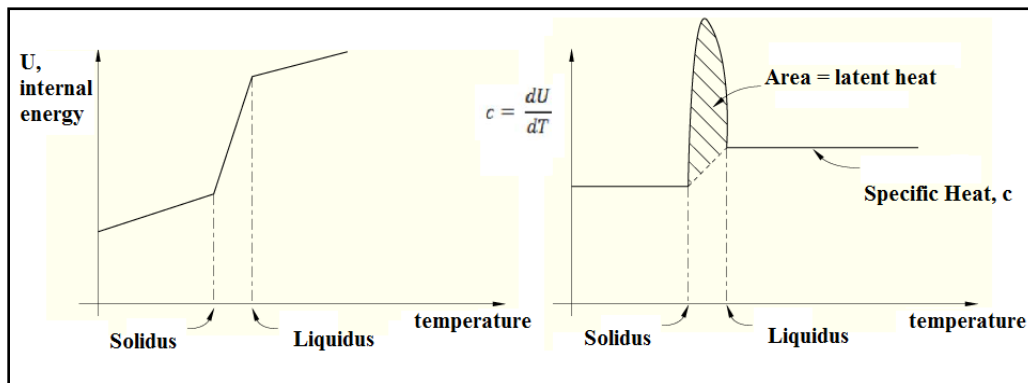


Figure 2-1: Sensible and Latent heat stored in PCM

Heat conduction is assumed to be governed by the Fourier law:

$$q_{hc} = -k * \frac{\partial T}{\partial x} \quad (2.2)$$

Surface convection is given by,

$$q_{sc} = h * (T - T_e) \quad (2.3)$$

Element types used in the current analysis are first order 4-noded quadrilateral heat transfer elements. ABAQUS use a numerical integration rule for first order elements where the integration points are the 4 corners of the quad element. The solutions in this case are non-smooth. This method is very effective when latent heat effects are considered since the jacobian term associated with the energy rate is diagonal. When second order elements are to be considered, ABAQUS uses the conventional Gaussian integration approach where the solutions are smooth. Since latent heat effects are to be accounted for which make the solution non-smooth, first order elements are preferred over second order elements in this case. A one-dimensional heat flow through the wall is assumed. However, a two-dimensional finite element model [Refer to Section 3.1] is used as shown in Figure 2-2 so that the same model can be used later to include flow through non-uniform walls such as those containing openings. ABAQUS Version 6.10 is used as the finite element program and it should be noted that the presence of a non-linear material (PCM) in the model necessitates a nonlinear, transient analysis. The wall height is taken as 1 m. Mixed boundary conditions are imposed on the outside and the inside faces. The ambient temperatures used as inputs to the model are obtained from reliable weather sources [43, 44]. The exterior convective heat transfer co-efficient, h_e is taken as 20 W/m²-°C and the interior convective heat transfer co-efficient, h_{int} is taken as 5 W/m²-°C [24, 45]. Instead of applying solar radiation as a flux on the outside face of the wall, in this study, a

temperature equivalent (T_{eq}) to radiation effect (during sunshine hours) is calculated as [24]:

$$T_{eq} = T_e + \frac{\alpha S}{h_e} \quad (2.4)$$

In the above equation, T_e is the ambient temperature without the radiation effects (in $^{\circ}\text{C}$), α is the absorption coefficient (unit less), S is the solar Insolation (defined as rate of delivery of solar radiation per unit area with units of kWh/m^2 per day), and h_e is the convective heat transfer coefficient, with units of $\text{W}/\text{m}^2\text{-}^{\circ}\text{C}$.

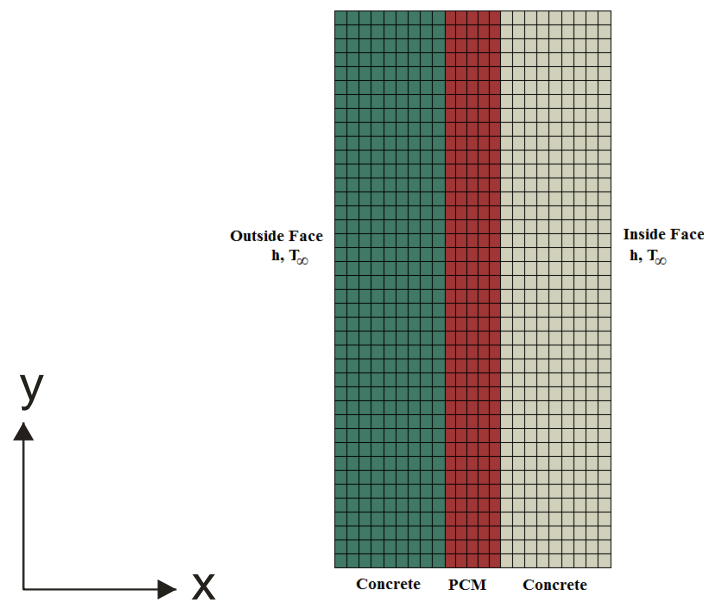


Figure 2-2: Finite element model (1 m high)

In addition it is assumed that: (a) all the concrete and PCM layers are homogenous and isotropic, (b) thermal properties of concrete and PCM are constant and temperature independent, (c) convective flow, if any, inside the liquid PCM is ignored, (d) there is no interfacial resistance between the layers, and (e) the top and the bottom surfaces are perfectly insulated. The air and the air

flow in the HVAC-controlled enclosure are not modeled. The initial temperature (when the analysis starts) of the entire wall is assumed to be the near the initial temperature of the inside face of the wall (which is governed by the controlled climate inside). First order, 4-noded quadrilateral elements (DC2D4) are used in all cases.

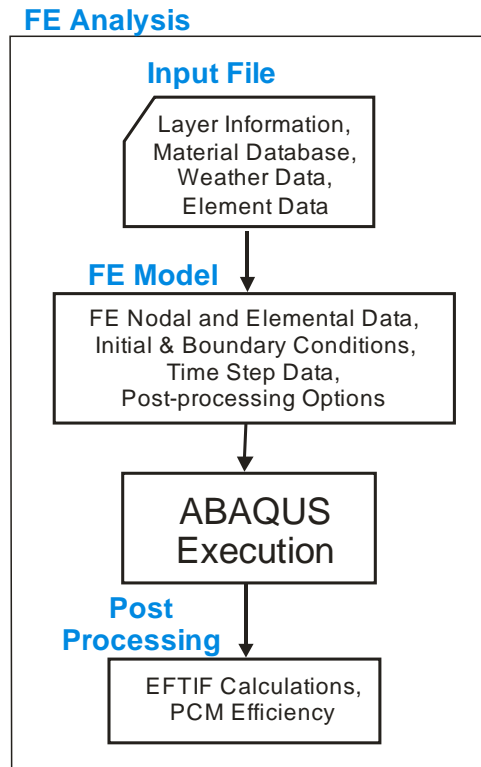


Figure 2-3: Computational framework for finite element analysis

To automate the FE model construction, analysis, and post-processing steps, an in-house custom-built framework (WallDesign) is used (See Figure 2-3). The framework controls the executions as follows. It first reads the problem input file and generates the finite element model, followed by the ABAQUS input file. ABAQUS is launched and the program waits for the normal completion of the ABAQUS run. It then reads the ABAQUS output file and carries out the required

post-processing steps. The existing framework can be readily extended to carry out further studies such as design optimization using an optimization toolbox. Detailed description of the WallDesign framework is shown in appendix A.

A convergence study was carried out to determine the optimal finite element model - one that would yield acceptably accurate results with the least amount of computational time. A uniform mesh was used in the study with the size of a typical element varying between 0.003 m and 0.01 m. A FE model containing a PCM layer was analyzed for a period of 7 days using time steps of 15 minutes, 30 minutes and 60 minutes with varying element sizes. The results indicate that the system response stabilized after the first 24 hours, generally showed a cyclic pattern, and the final results at the end of the week are consistent. Figure 2-4 shows the energy flow through inside face (EFTIF) value and Figure 2-5 shows the inside face temperature after 30 hours and 44 hours as a function of the element size. Both response measures show a nicely converging trend. Based on the results of the convergence study, the following model parameters were used in all subsequent finite element analyses: (a) element size of 0.5 cm, (b) 60 minute time step, and (c) for different duration of analysis the results are reported for the second 24 hours.

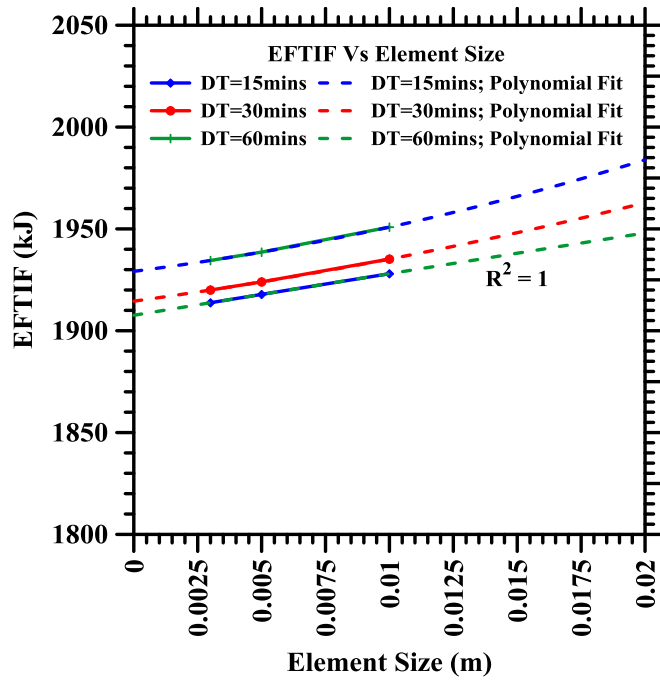


Figure 2-4: EFTIF versus element size

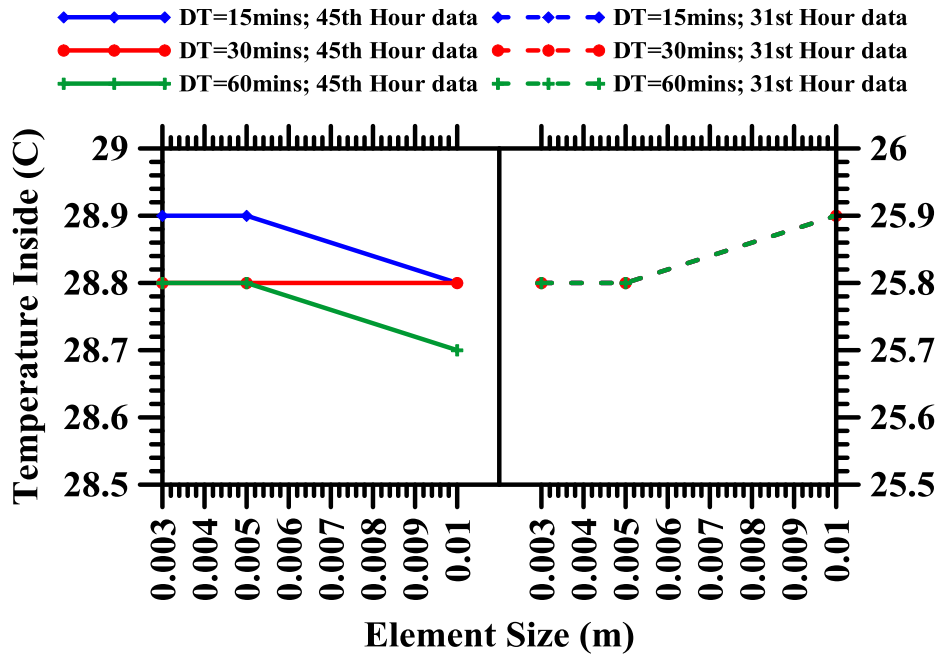


Figure 2-5: Inside wall temperature versus element size

Two performance metrics are considered when comparing different scenarios. They are:

- (i) Energy Flow Through the Inside Face (EFTIF): Heat flux values, τ_x (rate of heat energy transfer through a unit area) from the ABAQUS output file are used to compute energy flow through all the elements in the inside face (assuming unit depth) as:

$$EFTIF = E = \int_{t_i}^{t_f} \int_0^1 \tau_x dy dt \quad (2.5)$$

Where, t_i and t_f are the initial and final time values and 1 reflects the unit distance in the y-direction.

The energy flow can potentially take place from outside to inside or from inside to outside depending on the ambient temperature, because the indoor temperature is maintained within a desired range. In this study, EFTIF is the total energy flowing in both directions and represents a measure of the HVAC cost required to keep the air inside the building at the prescribed temperature range. An efficient passive system keeps the EFTIF minimum.

- (ii) PCM Efficiency (PCME): The energy stored in (or released from) the PCM is due to both the sensible and latent heat storage capacities of the PCM and they are computed as:

$$Q_s = \int_{T_i}^{T_f} m C_p dT \quad (2.6)$$

$$Q_L = m \Delta H_{PCM} \quad (2.7)$$

In the above equations, Q_s is the sensible heat storage capacity, Q_L is the latent heat storage capacity, m is the mass of the PCM or concrete, C_p is the specific heat capacity, and ΔH_{PCM} is the latent heat capacity of the PCM.

These expressions are evaluated for each time step (60 minutes) and their absolute values are summed over the time duration to compute the total energy value. The efficiency of the PCM is calculated based on the energy stored in the PCM at any given time as:

$$PCME = \frac{\text{Energy stored in PCM}}{\text{Energy storage capacity of PCM}} \times 100 \quad (2.8)$$

Since the cost of the PCM is a function of the amount of PCM used in the wall, the PCM characteristics that results in the maximum possible efficiency should be chosen.

3.0 PRELIMINARY STUDIES

This chapter focuses on study of analysis parameters and selection of the best configuration feasible. In section 3.1, results from preliminary studies of types of PCM have been discussed. Based on these results paraffins were chosen for analysis in the research work. In section 3.2, heat flow through a 10cm thick and a 20cm thick concrete walls embedded with 0-20% of PCM was studied and results presented. Purpose of comparison between the two different wall sections is to verify basic heat transfer rules. Conclusions from this particular analysis were useful in drafting problem statements for other analyses.

3.1 Selection of Suitable PCM

Not all PCMs can be used for thermal storage. Selection of a suitable PCM is probably one of the most important steps to this research. The most ideal PCMs would have the following properties:

- Suitable phase change temperature.
- High latent heat of fusion per unit mass.
- Good cycling stability without phase separation.
- High specific heat provides additional sensible heat storage.
- Little or no sub-cooling during freezing.
- Good thermal conductivity. Low price and good recyclability.
- Non-poisonous, non-flammable, non-explosive, non-corrosive and not subject to chemical decomposition.

Model Details and Material Properties

For the analysis reported in this section, six different types of PCMs are considered along with analysis of a plain concrete wall for low temperatures at the inside face of the wall and low EFTIF. The properties of all materials used have been listed in Table 3-1. The baseline wall configuration can be seen in Figure 3-1. The wall is 1m high and 0.2m wide, with a 1cm PCM layer embedded in the center of the wall. Ambient air temperature profile (applied to the outside face of the wall) and inside face air temperature (IFAT, applied to the inside face of the wall) for a typical day in Phoenix, AZ have been shown in Figure 3-2.

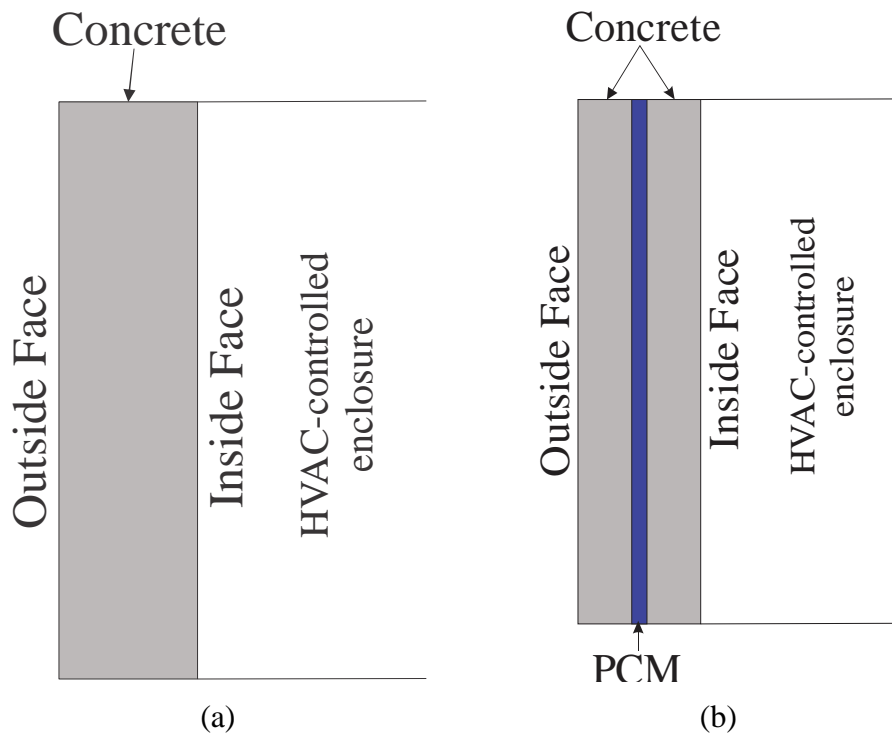


Figure 3-1: (a) Typical plain concrete wall, (b) Wall with a centrally placed 1cm PCM layer

Table 3-1: Material properties used in the analyses

Property	Type of PCM	Density	Specific Heat	Conductivity	Latent Heat	Phase Change Temperature (PCT)	
Units		kg/m ³	J/kg-°C	W/m-°C	kJ/kg	°C	K
Concrete	-	2400	750	1.45	-	-	-
PEG 600	PEG	1126	2135	0.2	146.5	15 - 25	288 - 298
Paraffin	Polyethylene C _n H _m	800	25000	0.35	245	27.5 - 29	300.5 - 302
Microencapsulated PCM (MEP)	Paraffin	800	2400	0.2	169	27 - 31	300 - 304
Capric Acid (CA)	Fatty acid	1000	1900	0.149	153	31 - 33	304 - 306
CaCl	Inorganic salt	1700	3020	1.0	190	29 - 31	302 - 304
Butyl Stearate (BS)	Stearic acid butyl ester	850	1386	0.2256	140	18 - 20	291 - 293

Numerical Results

Figure 3-2 shows variation of the temperature of the inside face of the wall with respect to time. Highest inside temperatures can be seen in case of a plain concrete wall and lowest inside temperatures can be seen for paraffin and PEG 600 during daytime. At nighttime higher inside temperatures are seen when paraffin and PEG 600 are used. This is most desirable and clearly use of either polyethylene paraffins or PEG 600 is most beneficial.

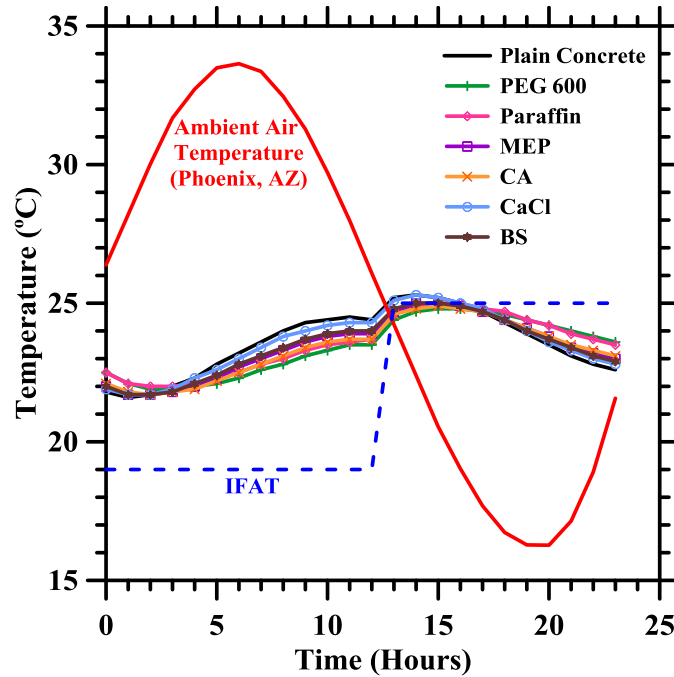


Figure 3-2: Comparison of temperature variation at the inside face of concrete wall

It is also seen that incorporation of PCM into the wall system introduces a time lag for the peak ambient temperature (occurring at 6 hours) reaching the inside face of the wall. Smallest time lag is seen with plain concrete and CaCl as PCM (8 hours) and highest lag is seen with paraffin and PEG 600 (9-10 hours). A

higher time lag is more desirable since, it delays the maximum amount of heat reaching the inside face to nighttime when it is desirable to keep inside temperatures above the ambient temperature (within the IFAT range).

Similar conclusions can be drawn by studying the EFTIF of the wall (Refer Figure 3-3). Highest EFTIF is seen in case of plain concrete, CaCl and lowest for again PEG 600 and paraffin. The drop in EFTIF values during the 13th – 14th hour is due to change in transition of ambient temperature from above the IFAT range to below the IFAT range.

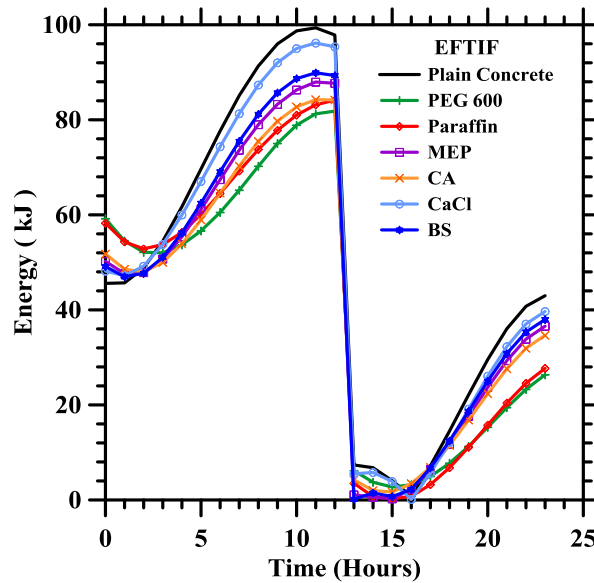


Figure 3-3: Comparison of EFTIF of concrete wall

In order to avoid some problems inherent with inorganic materials, researchers have turned towards some of the materials from the organic class, like PEG's, fatty acids and paraffins [20]. Various studies have concluded that amongst all the classes of PCMs, paraffins comply with most of the above selection criteria [46, 47]. As seen in the results paraffins and PEG's seem to be better suited for our current analysis purpose.

Hence, considering cost benefits, suitability and ease of availability four commercially available paraffins were chosen for the purpose of current research work [48, 49, 50]. The PCMs used here forth, PCM A, B, C and D [26], are all organic paraffins with molecular formula C_nH_m ($m = 2n+2$ in case of PCM A). Both PCMs have a low thermal conductivity and higher enthalpy of fusion. The temperature of phase change for both PCMs is suitable for the ambient temperature range for locations considered herewith.

3.2 Comparison between 10cm and 20cm thick walls

Current section deals with comparison of a 10cm thick wall and a 20cm thick wall with same % by volume of PCM layer (PCM A) sandwiched in between. The same FEA model as used in section 3.2 has been considered for this analysis with the distinction of wall thickness. Weather data of the hot day in Phoenix (June 14th 2011) is used for the purpose of this comparison as can be seen in Figure 3-4.

Table 3-2 – Material Properties

Property	Units	Concrete	PCM-A
Density	kg/m ³	2400	800
Specific Heat	J/kg-°C	750	2400
Conductivity	W/m-°C	1.45	0.2
Latent Heat	kJ/kg	-	169
Phase Change Temperature (PCT)	°C	-	27 – 31
	°K	-	300 – 304

Numerical Results

Table 3-3 shows values of EFTIF, energy savings, maximum sensible and latent energy stored for different percentages of PCM A placed centrally in a concrete wall. All reported results are for the second 24 hour period. Energy savings increase with increasing PCM percentage in both cases. Savings obtained with a 10cm thick wall is approximately 45-55% of savings obtained with 20cm thick wall (for the same % of PCM).

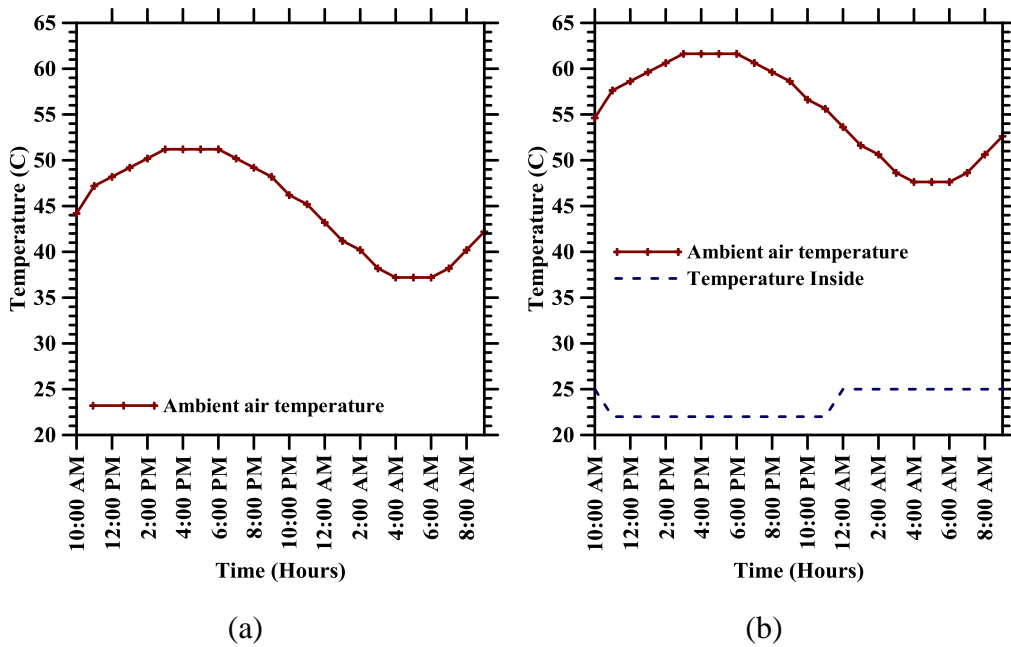


Figure 3-4: Ambient air temperature profile for Phoenix, AZ: (a) without radiation effects, (b) with radiation effects

Table 3-3: EFTIF data summary for section 3.3

Thickness (concrete wall)	% of PCM	Thickness	EFTIF	Savings	Max. Sensible Energy	Max. Latent Energy	Cost of 1m x 1m section
		(cm)	(kJ)	%	(kJ)	(kJ)	\$
10cm	0	0	6138		0	0	50
	5	0.5	5749	6	177	676	65
	10	1	5407	12	347	1352	81
	15	1.5	5103	17	509	2028	96
	20	2	4832	21	667	2704	111
20cm	0	0	5046		0	0	101
	5	1	4540	10	310	1352	131
	10	2	4124	18	604	2704	161
	15	3	3767	25	885	4056	191
	20	4	3420	32	1151	5408	222

EFTIF decreases with increasing PCM mass and is higher for a 20cm thick wall with PCM than for a 10cm thick wall with the same % of PCM (Refer Figure 3-5). It can be seen that a pure 20cm thick wall results in approx. the same amount of EFTIF as for a 10cm thick wall with 1.6cm PCM. Hence, to match EFTIF flow through a 10cm thick wall to that through a 20cm thick wall, a minimum of 1.6cm thick PCM layer is needed. In other words, instead of using a 20cm thick pure concrete wall, a 10cm thick concrete wall embedded with 1.6cm PCM may be used (where allowable by design constraints), which will ensure cost savings.

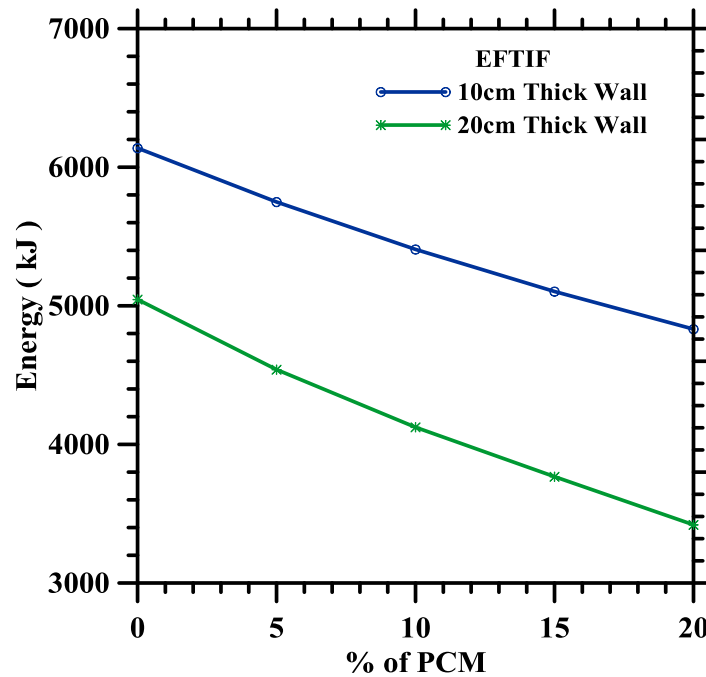


Figure 3-5: EFTIF w.r.t. % of PCM in wall

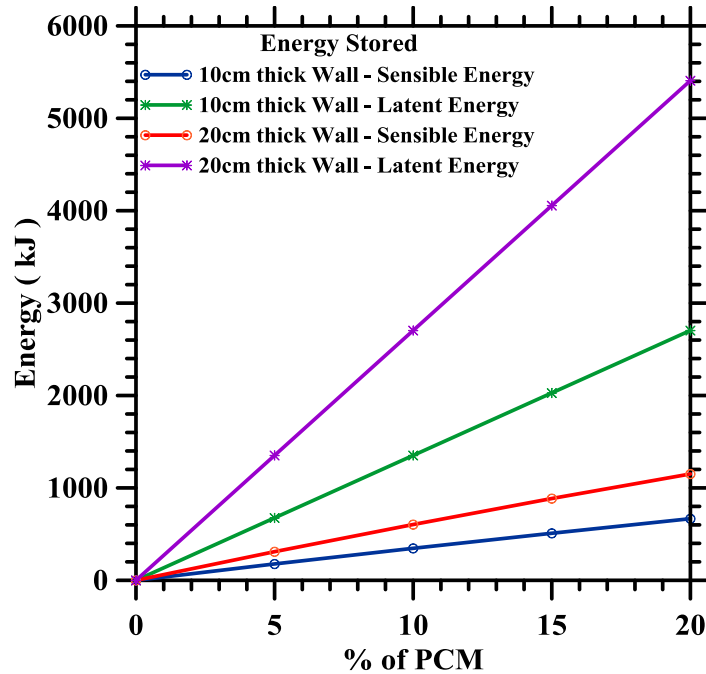


Figure 3-6: Maximum energy stored in PCM

Again as seen in Figure 3-6 energy stored in PCM increases with increasing PCM mass. For the same % of PCM (w.r.t. wall thickness) energy stored by PCM is higher in case of 20cm thick wall, which is due to higher mass of PCM.

Summarizing, temperature of inside face decreases with increasing PCM thickness when ambient temperature is higher than IFAT and increases with increasing PCM thickness when ambient temperature is lower than IFAT. EFTIF decreases and savings increase with increase in PCM mass for any model including PCMs. Savings obtained from 10cm thick wall are half those from a 20cm wall. A pure concrete wall 20cm thick has the same energy saving effects as a 10cm thick concrete wall embedded with 1.6cm thick PCM layer at the center.

4.0 EFFECT OF VARYING PCM THICKNESS AND AD-HOC OPTIMIZATION

This chapter focuses on effect of variation of PCM thickness, PCM location and varying boundary conditions on study parameters. Only a single PCM layer has been studied. Widening scope of this review further, effect of changing PCM properties is also considered. An ad-hoc optimization is carried out (keeping the PCM thickness constant) and its significance observed. This can be used as a guideline for future optimization studies.

4.1 Typical wall geometry and layout

The baseline wall configuration is shown in Figure 4-1(a). The total wall thickness is taken as 20 cm (8 in, which corresponds to typical precast concrete structural wall thickness for industrial and high rise buildings) for all the analysis cases in this paper. One of the scenarios considered in this study, a centrally located PCM layer, is shown in Figure 4-1(b). The PCM thickness is varied between 1 and 5 cm. In other words, 5-25% of the wall volume is occupied by the PCM. The higher end values are not always practical when one considers the cost of the PCM, but is included in this analysis because the aim is to understand the influence of PCM volume (or layer thickness) on the thermal efficiency of the wall system. Furthermore, the analysis also considers an exceptionally hot climate, which necessitates a larger amount of TES material to achieve desirable performance levels. The outside face of the wall is exposed to the sun. The inside face is exposed to air whose temperature is controlled by a heating, ventilation

and air-conditioning (HVAC) system. This temperature is referred to as inside face air temperature (IFAT) in the rest of the paper.

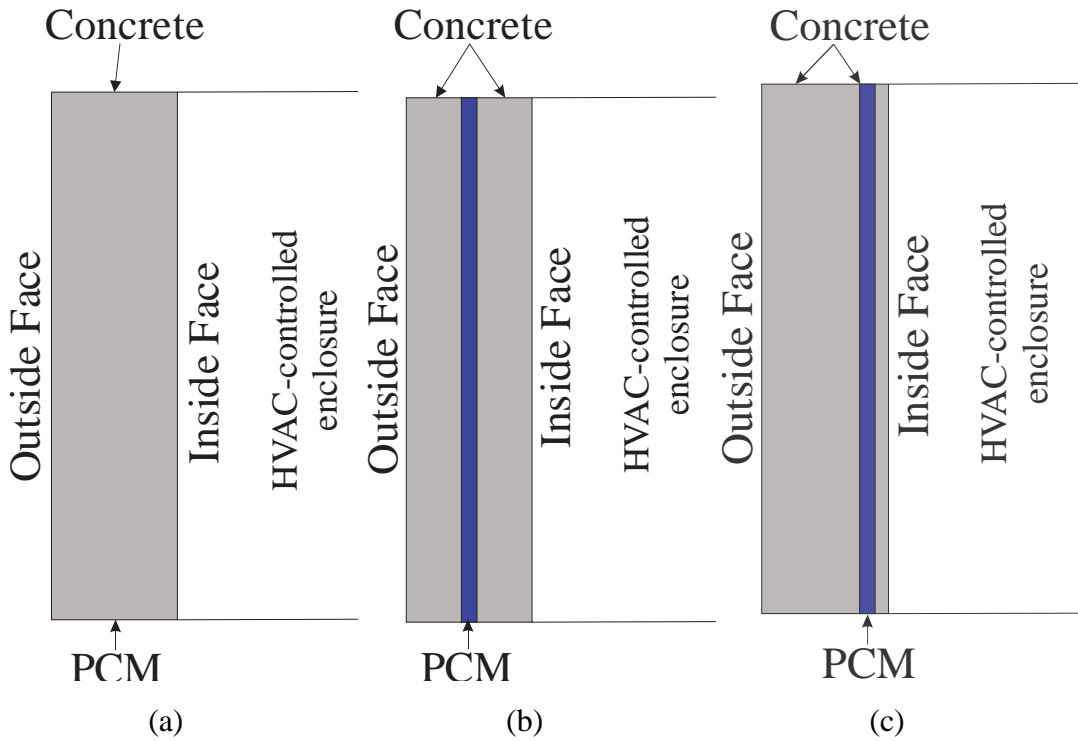


Figure 4-1: (a) Typical concrete wall, (b) Wall with a centrally placed PCM layer, and (c) PCM layer placed closer to the inside face

4.2 Concrete and PCM properties

For the analyses reported in this paper, two types of concrete – normal weight and light weight (NC and LWC respectively) are chosen. Lightweight aggregates are used to produce lightweight concrete, and a density reduction in the range of 15-30% is generally achieved. This has implications in the heat transfer properties of the structural member. Additionally, the reduced density of the structural system results in economical design of supporting elements. The relevant physical properties of concrete are given in Table 4-1.

Table 4-1: Material properties used in the analyses

Property	Units	NC	LWC	PCM-A	PCM-B
Density	kg/m ³	2400	1750	800	300
Specific Heat	J/kg-°C	750	960	2400	2500
Conductivity	W/m-°C	1.45	0.64	0.2	0.25
Latent Heat	kJ/kg	-	-	169	110
Phase Change Temperature (PCT)	°C	-	-	27 – 31	22 – 25
	°K	-	-	300 – 304	295 – 298

Two types of PCMs are used, referred to as PCM-A and PCM-B in this study, the properties of which are also provided in Table 4-1. Both these PCMs are microencapsulated paraffins, and thus relatively cost-effective and easy to use. The molecular weights of these paraffins as well as their encapsulation methodology are different, which results in changes in their material properties as shown in Table 4-1.

4.3 Ambient temperature data

The 24-hour variations in temperature for the two chosen locations are shown in Figure 4-2. The maximum temperature change during the 24-hour period is 5°C for Los Angeles and 14°C for Phoenix. It should be noted that weather data is available at a minimum frequency of 15 minutes. Instead of

applying solar radiation as a flux on the outside face of the wall, in this study, an equivalent temperature (T_{eq}) is calculated (Refer Equation (2.4)).

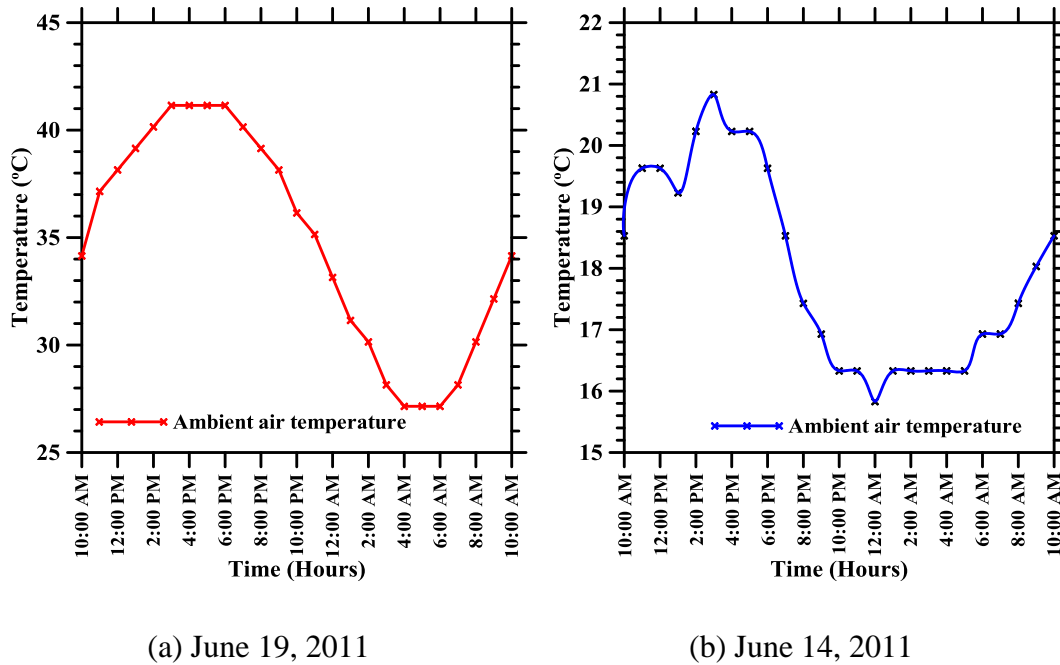


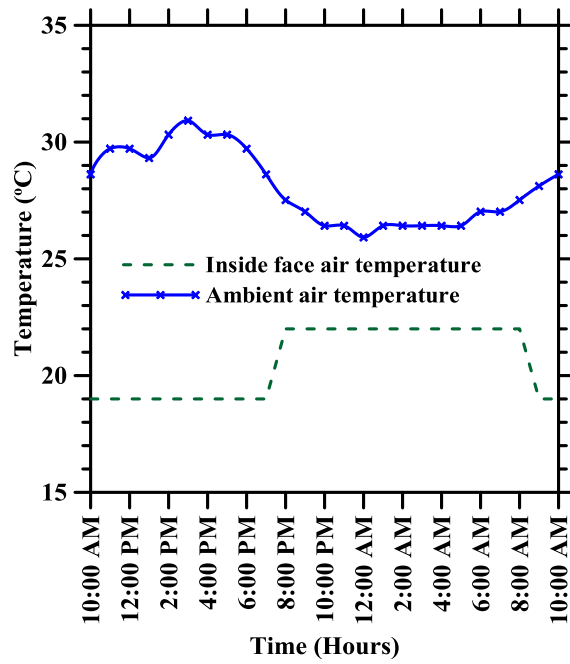
Figure 4-2: Ambient air temperature profile [43]: (a) Phoenix, (b) Los Angeles

The values for the coefficients which are used in the equation, for the analyses reported in this study are shown in Table 4-2. Note that the solar Insolation values for Los Angeles and Phoenix are very close to each other, potentially because of the same latitude in which both the cities lie. The computed additive component to the ambient temperature, which accounts for the radiation effects [51, 52], is therefore similar for both the cities (10.1°C for Los Angeles and 10.0°C for Phoenix).

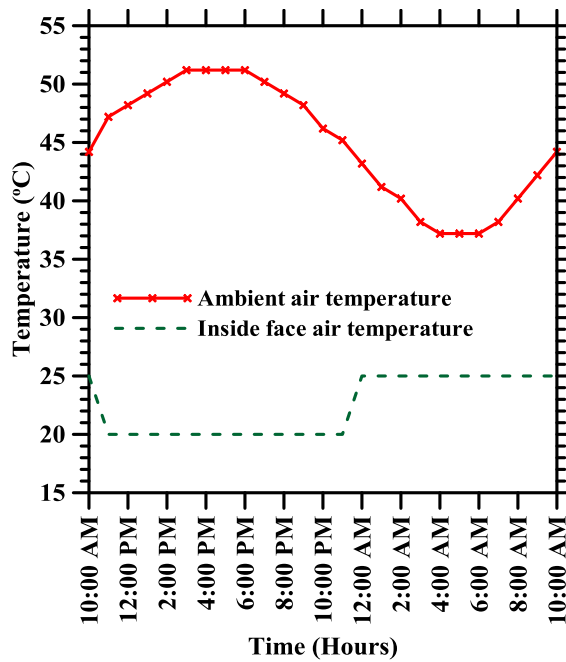
Table 4-2: Radiation-related Data

Location	Solar Insolation (S)	Absorption Coefficient	Convective heat transfer coefficient: outside face (h_e)	$\alpha S/h_e$
	(W-s/m ² /s)	(α)	(W/m ² °C)	(°C)
Los Angeles	310.4	0.65	20	10.1
Phoenix	309.2	0.65	20	10.0

The effective ambient temperature profiles that include the equivalent radiation effects are shown in Figure 4-3, where the inside face air temperature (IFAT) is also shown. During the day hours (10 AM to 8 PM), IFAT for Los Angeles is taken as 18.9°C and during the rest of the time (9 PM to 9 AM) is taken as 21.9°C. Slightly different IFAT values and timings are used for Phoenix - a temperature of 19.9°C from 11 am to midnight and a temperature of 24.9°C from 1 AM to 10 AM. The differences in timings and temperatures are chosen so as to reflect differences between the two locations. Phoenix has: (a) a drier climate (lower humidity) than Los Angeles permitting a higher indoor target temperature with the same comfort level, and (b) a higher evening temperature and the night time cooling takes place very gradually. Effectively there is a maximum difference of 9°C for Los Angeles and 26°C for Phoenix between the outside air temperature and IFAT. It is evident that the energy requirements to maintain indoor comfort levels would then be different between these two locations, resulting in different PCM incorporated structural element design strategy.



(a)



(b)

Figure 4-3: Ambient air temperature profile with radiation effects for: (a) Los Angeles, and (b) Phoenix. IFAT is also shown for both the cases.

4.4 Results from Numerical Analysis

The PCM layer is positioned at the center of the wall and the PCM layer thickness is varied between 0 and 5 cm with 0 cm being the baseline model (concrete only). The performance of the wall system where the primary component is normal concrete (NC) or light weight concrete (LWC) is considered. For each model, we calculate the following parameters over the second 24-hour period (starting at 10 AM): (a) the temporal change in temperature of the inner face, (b) EFTIF, and (c) PCME. We present details of the analysis and results only for Phoenix (to keep the discussions succinct) while the overall performance of the wall in both Los Angeles and Phoenix are compared at the end of this section.

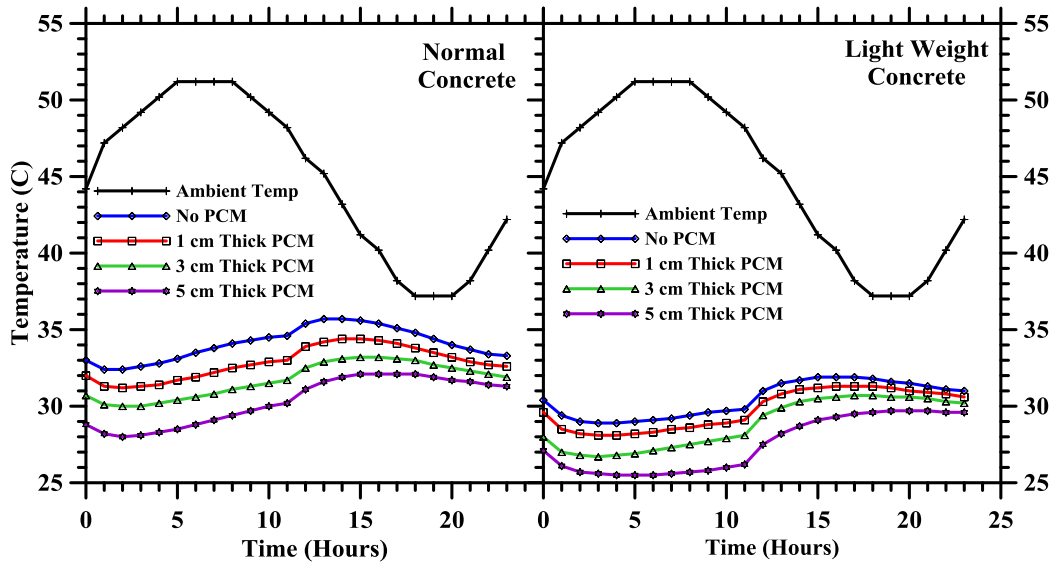
4.4.1 PCM for Phoenix

In this section we present and discuss the results for Phoenix with the FE model boundary conditions as described before. The external temperature profile is shown in Figure 4-3 and the model layout is shown in Figure 4-1. PCM-A is considered an appropriate choice for Phoenix since its Solidus-Liquidus temperature range is within the desired indoor air temperature range.

Temperature variation on the inner face of the wall

Figure 4-4 shows the variation of the temperature of the inside face as a function of time for NC and LWC walls. The results shown here indicate the influence of PCM thickness and concrete type on the temperature of the inside face of the wall. With a much higher difference in temperature between the

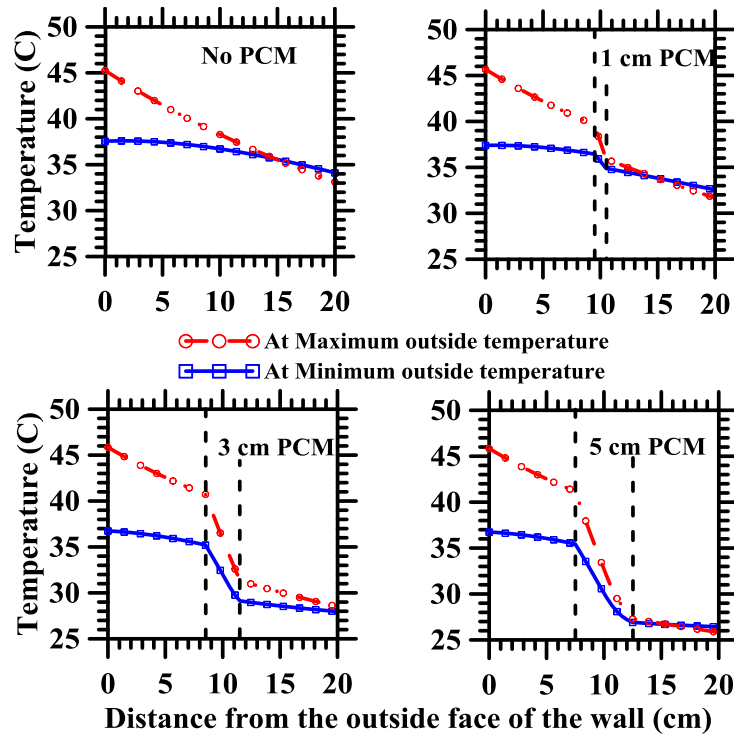
outside ambient air and inside face air temperature as in the case of Phoenix, the maximum temperature differences between the baseline configuration and the wall with 5 cm PCM are 5°C and 4°C for NC and LWC walls respectively. Needless to state, this is a significant change, which will impact the energy efficiency of the structure. For the same ambient temperature impulse, the lightweight concrete walls with and without PCM result in lower temperatures, in the range of about 2°C, in the inside face as compared to normal concrete walls. This is an expected response accounting for the thermal characteristics of lightweight concrete systems. For normal concrete, the maximum temperature difference on the inside face of the wall is between 3-4°C for all four scenarios (no PCM, 1, 3 and 5 cm PCM), and for the lightweight concrete wall, the temperature difference is about 2-4°C. Another point to note from these figures is the relatively linear reduction in temperature of the inside face with increase in PCM thickness. This is an indication that, in the chosen range of boundary conditions and material parameters, the PCM layer reaches its energy absorption capacity fairly quickly and further energy absorption is facilitated by an increase in PCM thickness. From a structural-thermal-cost viewpoint, a detailed optimization exercise for PCM type and thickness is necessary, which is the focus of an upcoming paper by the authors.



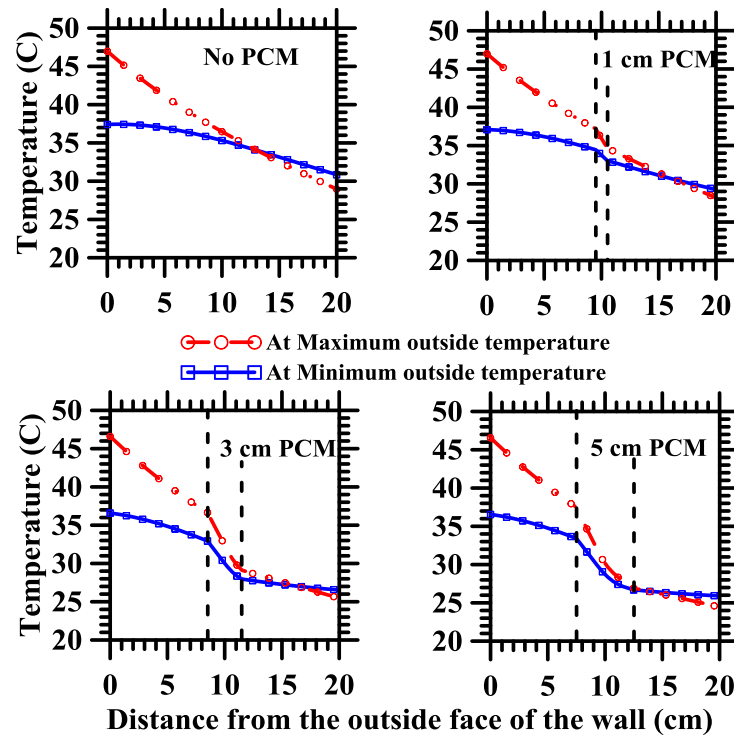
(a) (b)

Figure 4-4: Temperature variation as a function of time at the inside face of the wall for ambient conditions corresponding to Phoenix: (a) NC, (b) LWC. The results shown are for PCM-A.

Figure 4-5 shows the temperature profile through the wall with respect to thickness (0 is the outside face and 20 cm is the inside face) for the times of day when the outside air temperature is at their maximum (4:00 PM) and the minimum (5:00 AM) values - a snapshot in time to compare the different scenarios. The temperature of the inside face is between 26°C (5 cm PCM) and 34°C (no PCM) for the different thicknesses of PCM when NC is used and between 24°C (5 cm PCM) and 31°C (no PCM) when LWC is used. The thermal gradient is much steeper through the PCM (more so for the thicker PCMs). This is to be expected as the PCM layer absorbs energy and delays the heat flow into the inner layer of concrete.



(a)



(b)

Figure 4-5: Temperature variation through the wall: (a) NC, (b) LWC

Energy flow through the inner face of the wall

Figure 4-6 depicts the energy flow through the inner face of the normal and lightweight concrete walls. It is observed that EFTIF decreases with increasing PCM thickness. The performance of LWC is better than NC by as much as 32% when a PCM layer thickness of 2 cm PCM used. The relationship between energy flow and PCM thickness is mildly nonlinear for both the cases, even though a linear approximation would suffice to explain the system response. For both NC and LWC, the EFTIF values for a wall with 5 cm thick PCM layer are only 40% of that of the baseline case. Based on the modeled energy flow and using the specified ambient outdoor and the desired indoor temperatures, this type of analysis can help determine the optimal PCM layer thickness, keeping other considerations also in mind.

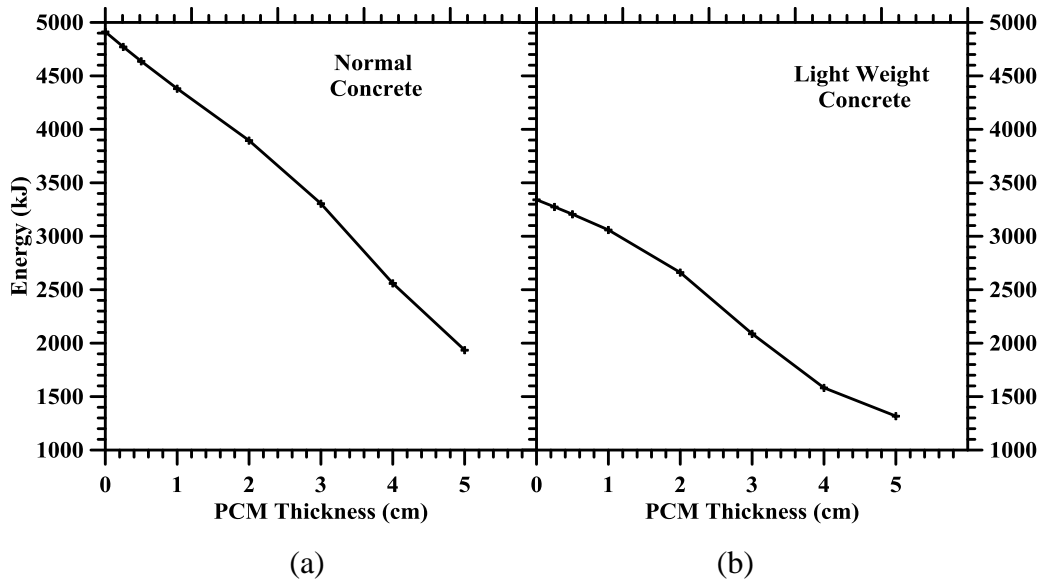


Figure 4-6: Energy flow through inner face versus PCM thickness:

(a) NC, (b) LWC

In Figure 4-7, EFTIF is represented as a function of time for the normal and lightweight concrete walls. Each graph shows two zones – one corresponding to the daylight hours when energy demand to cool the inside air is high, and the other corresponding to the night time when energy demand is relatively lower. As before, the energy differences between the cases with or without PCM are higher for normal concrete walls as compared to lightweight concrete walls. The drop in EFTIF values after 12 hours can be attributed to the higher IFAT values at night. Since the difference between the ambient and IFAT temperatures is lower at night, there is lesser thermal load to handle by the wall/PCM and hence lower EFTIF values are observed.

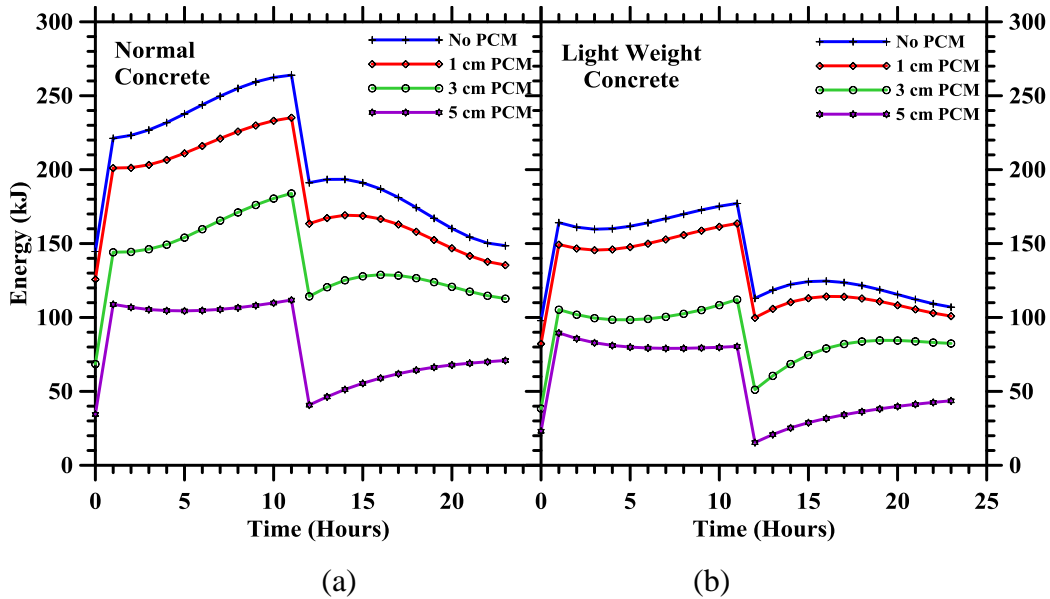


Figure 4-7: Energy flow through inner face with respect to time: (a) NC (b) LWC

The effect of LWC is prominent only at lower PCM thicknesses. In other words, the EFTIF values are almost the same for 5 cm thick PCM regardless of the type of concrete. It is noticed that the difference in the EFTIF values between

walls with 1 cm and 3 cm thick PCM is larger than those between walls with 3 cm and 5 cm PCM. The latent heat storage capacity of the PCM becomes dominant at higher PCM thicknesses, making the concrete type less significant. This has direct implications in the choice of the host system. If it is possible (from an economy and structural standpoint) to have higher volumes of PCMs in the structural system, it is not imperative to choose a concrete with optimal thermal properties. In other words, it is unnecessary to incur extra cost on lightweight aggregates solely from a total energy flow standpoint if the PCM volume fraction in the wall system is going to be large enough to attain the required thermal characteristics. Analyses such as those presented in Figure 4-7 can help the designer to optimize the material design in such cases.

Energy stored in PCM

Figure 4-8 and Figure 4-9 show the cumulative sensible and latent heat energies respectively, stored in the PCM as a function of time. While the energy stored in the PCM (latent and sensible energy) increases with increasing PCM content, the contribution from sensible energy is overshadowed by the latent heat storage capacity of the PCM. The higher thermal resistance of LWC delays the heat flow reaching the PCM layer and hence the latent energy stored in the LWC wall with PCM is about 10% lower compared to the NC wall with PCM. The PCM absorbs energy from about 10 AM to 11 PM and then starts releasing the energy till about 8 AM. This behavior is much more pronounced: (a) as the PCM thickness increases, and (b) in NC compared to LWC. Lower PCM thicknesses result in lower energy storage capacities and hence the fluctuation in energy

storage is a function of the PCM capacity. With higher thicknesses, more energy can be stored in the PCM as a result of which the energy storage and release is much more distinct. Again, since the thermal resistance of LWC is more than NC, PCM in NC is subjected to increased heat transfer, which causes more fluctuation in energy storage in the PCM in the case of NC.

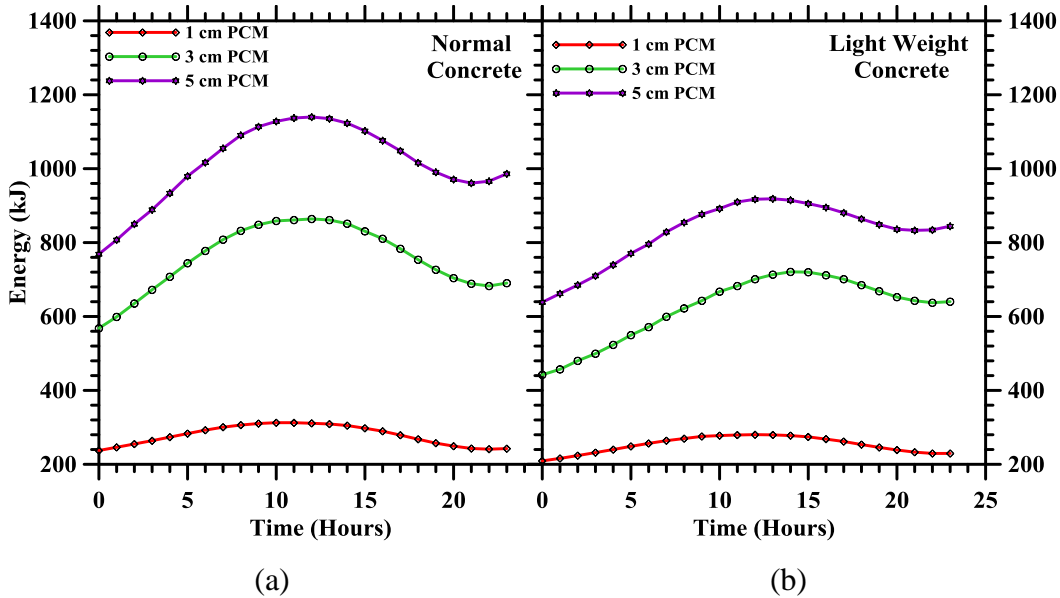


Figure 4-8: Cumulative sensible energy stored in PCM as a function of time: (a) NC, (b) LWC

The temperature of PCM layer in the NC walls with 1 cm and 3 cm thick PCM layers is entirely above the Liquidus temperature throughout the time period, and hence there is no change in the latent heat energy stored in the PCM as shown in Figure 4-9. However, for the wall with 5 cm thick PCM (NC), the latent heat energy continues to increase for the next 21 hours before leveling off. The LWC scenario shows that the 5 cm thick PCM at the end of the 24-hour period has additional energy storage capacity (see Figure 4-9). As stated earlier, lower thermal resistance of the NC leads to higher heat flow across the PCM

layers embedded in a NC wall. Hence, the amount of energy stored in the PCM is higher for wall with NC than for the wall with LWC, i.e., the PCM layer in a NC wall gets saturated earlier than a similar layer in LWC.

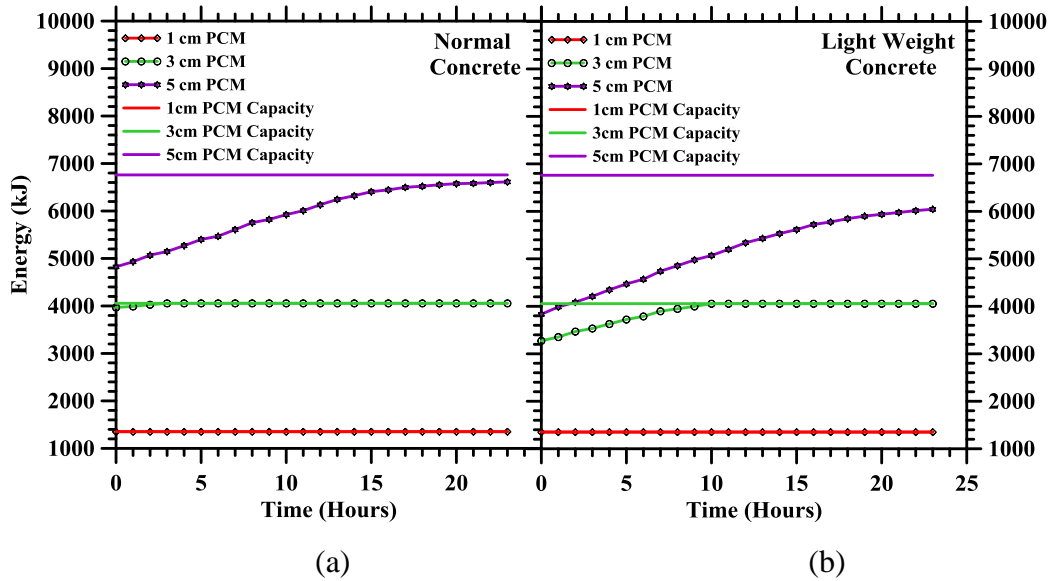


Figure 4-9: Cumulative latent energy stored in PCM as a function of time: (a) NC, (b) LWC

Figure 4-9 also shows the maximum PCM efficiency (PCME). The horizontal lines in these figures show the total latent heat energy capacity of the PCM layer. PCME is approximately 100% for both cases for the walls with 1 and 3 cm PCM thicknesses. Only the case with 5 cm thick PCM shows less than 100% efficiency indicating that there is excess latent heat storage capacity. However, at later times, the efficiency of the wall with 5 cm thick PCM layer also approaches 100%. This approach shows that, based on the desired IFAT and the desired reduction in HVAC costs (which depends on the energy flow across the wall), optimization of PCM thickness can be accomplished.

Effect of changing the PCM location

In the first step, the role of PCM location is studied. The PCM layer is shifted close to the outside face, referred to as PCM-Outer, or close to the inner face, referred to as PCM-Inner (Figure 4-1(c)). The FE model boundary and initial conditions are the same as that used in the centrally-placed PCM models. Table 4-3 summarizes the results for Phoenix (PCM-A).

Table 4-3: EFTIF Summary Table for Phoenix (PCM-A)

PCM-A Thickness (cm)	PCM-Outer		PCM-Center		PCM-Inner	
	EFTIF (kJ)	% decrease	EFTIF (kJ)	% decrease	EFTIF (kJ)	% decrease
0.0	4912	-	4912	-	4912	-
1.0	4372	11.0	4381	10.9	4379	10.9
2.0	3886	20.9	3896	20.9	3883	21.0
3.0	3374	31.3	3305	33.3	3189	35.1
4.0	2673	45.6	2560	48.5	2425	50.6
5.0	1989	59.5	1935	61.1	1896	61.4

In this case, there is very little difference in EFTIF when the PCM location is moved around. The perceptible differences (about 4-5 percentage points) are for the model with PCM layer thicknesses of 3-4 cm. In this case, the placement of PCM layer closer to the inside face of the wall is marginally more energy efficient. This is because of the delayed exposure of the PCM layer to the heat energy that is flowing into the wall. The thermal mass of a larger portion of concrete that facilitates this delayed exposure results in the PCM exposure starting only after a considerable part of high energy daylight hours. This results

in the PCM layer consuming more time to get fully saturated (i.e., complete the phase transition which stores the energy), thereby reducing the energy flow through the inside face of the wall. While this aspect does not get utilized for the 1 cm thick PCM case (layer saturation happens fast because of the low thickness), for the large PCM layer thickness (5 cm), complete layer saturation might not be happening.

4.4.2 PCM for Los Angeles

Table 4-4 summarizes the results for Los Angeles (PCM-B) using the same model and similar BCs with weather data from Los Angeles (refer Figure 4-3). For both locations similar results are seen. Changing the PCM location does not affect the EFTIF incredibly. Energy savings obtained in a PCM embedded wall with respect to a pure concrete wall are lower than those obtained for Phoenix (PCM-A).

Table 4-4: EFTIF Summary Table for Los Angeles (PCM-B)

PCM-B Thickness (cm)	PCM-Outer		PCM-Center		PCM-Inner	
	EFTIF (kJ)	% decrease	EFTIF (kJ)	% decrease	EFTIF (kJ)	% decrease
0.0	1636	-	1636	-	1636	-
1.0	1494	8.7	1494	8.6	1488	9.1
2.0	1363	16.7	1357	17.1	1342	18.0
3.0	1227	25.0	1215	25.7	1201	26.6
4.0	1089	33.4	1079	35.0	1069	34.6
5.0	961	41.3	954	41.7	947	42.1

4.4.3 Ad-hoc optimization for thermal efficiency

In order to better understand the role of PCM in achieving thermal efficiency, an ad-hoc optimization procedure is carried out where the PCM thickness is fixed and the properties are varied. Only NC is used in this optimization exercise.

Effect of changing PCM properties

In the second step, ad-hoc optimization is carried out to determine the optimal PCM material property combination (for the centrally placed PCM) assuming that the material parameters (identified in Table 4-5 with column heading as *Original*) can be varied $\pm 10\%$. The Phase change temperature (PCT) range, thermal conductivity, mass density, latent heat capacity (LHC) and specific heat capacity (SHC) are the parameters that are subjected to this change. It is evident that the energy efficiency can be improved by reducing the difference between the inside wall temperature and IFAT. Typically this can be achieved by: (a) decreasing the thermal conductivity (or increasing thermal resistance) that reduces the energy flow into the inside face of the wall, (b) increasing the mass density, latent heat capacity and specific heat capacity that all increase the ability of the PCM to store and release larger amount of energy, and (c) increasing the PCT range. This idea is used in the ad-hoc optimization scheme reported here. For the 1 cm PCM case, the original configuration is compared against a configuration where the PCT, LHC, SHC and density values are increased by 10% and conductivity is decreased by 10% (identified as *Combination 1-1*). Similarly, for the 5 cm PCM case, the original configuration is compared against

two configurations - in *Combination 5-1* the PCT, LHC, SHC and density values are increased by 10%, and conductivity is decreased by 10%; *Combination 5-2* is the same as *Combination 5-1* except that the PCT values are left unchanged (same as the original configuration). The results are summarized in Table 4-5.

For the 1 cm thick PCM layer (*Combination 1-1*), overall energy decrease is hard to achieve with the range of available values. An insignificant reduction (2%) is achieved by decreasing the thermal conductivity, and increasing the mass density, LHC, SHC and PCT. However, with the 5 cm thick PCM layer (*Combination 5-2*), better thermal efficiency is achieved.

A much larger decrease in EFTIF, of 17%, is observed. Understandably, changing the properties of PCM in a thicker layer is more effective. When the PCM efficiencies are determined in accordance with Equation 5, the *Combination 5-1* shows a PCME of only 69% showing that the latent energy storage capacity is not fully utilized in this case. This is because the phase change temperature (29.7-34.1°C) is higher in this case as compared to the original scenario (27-31°C). In contrast, the original and *Combination 5-2* cases have lower PCTs, resulting in PCMEs of 98% and 91% respectively.

Table 4-5: Ad-Hoc Optimization for Centrally Placed PCM Model (Phoenix).

The beneficial combinations as far as EFTIF is concerned, is shaded.

	Original	<i>Combination 1-1</i>	Original	<i>Combination 5-1</i>	<i>Combination 5-2</i>
PCM-A Thickness (cm)	1.0	1.0	5.0	5.0	5.0
PCT (°C)	27-31	29.7-34.1	27-31	29.7-34.1	27-31
PCT (K)	300-304	302.7-307.1	300-304	302.7-307.1	300-304
PCT range (°C or K)	4.0	4.4	4.0	4.4	4.0
Conductivity (W/m °C)	0.2	0.18	0.2	0.18	0.18
Density (kg/m ³)	800	880	800	880	880
LHC (kJ/kg)	169	185.9	169	185.9	185.9
SHC (J/kg °C)	2400	2640	2400	2640	2640
EFTIF (kJ)	4381	4286	1935	2025	1603
Normalized EFTIF	1.0	0.978	1.0	1.047	0.828

Figure 4-10 shows the temporal performance of *Combination 5-2* with respect to EFTIF, temperatures in the outside and inside faces, and the temperatures at the extremities of the PCM layer. After the initial 24-hour period (which is not shown in the graph because the analysis uses the second 24 hours as explained earlier), heat flows consistently into the inside enclosure, the magnitude of which varies between 24 kJ and 104 kJ.

The peak flow occurs during daytime hours, drops off at the start of the night time hours and gently increases thereafter. One important feature to note in this graph is the closeness of the values of the inside wall face temperature and the temperature of the inner interface of the PCM-concrete layer. This is ample demonstration of the effect of energy storage in the PCM whereby the inner face temperature does not go up significantly. The scenario where the inner face temperature closely follows the IFAT would be the ideal one as far as minimization of HVAC energy input is concerned. The finite element framework described in this paper is capable of simulating a variety of possible scenarios, and arriving at sensible structural-thermal-economic decisions.

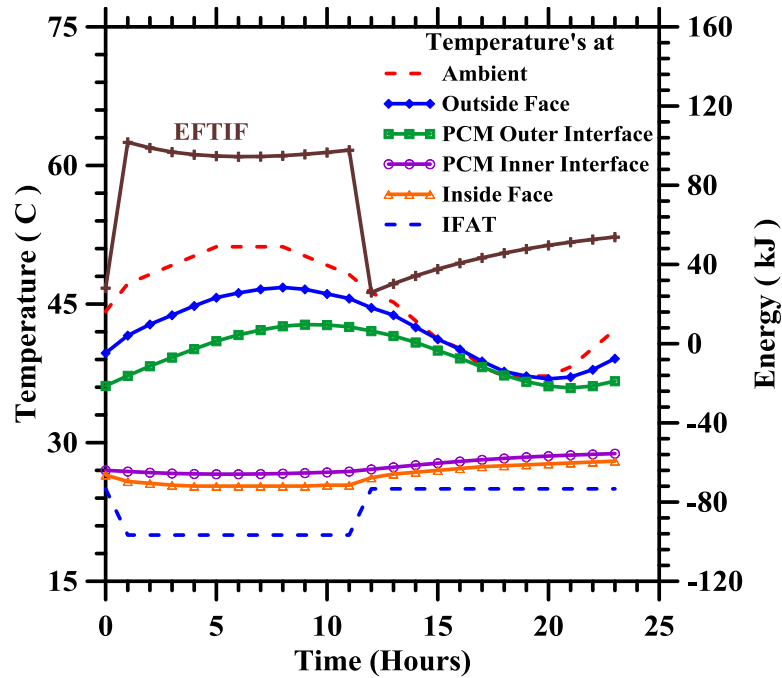
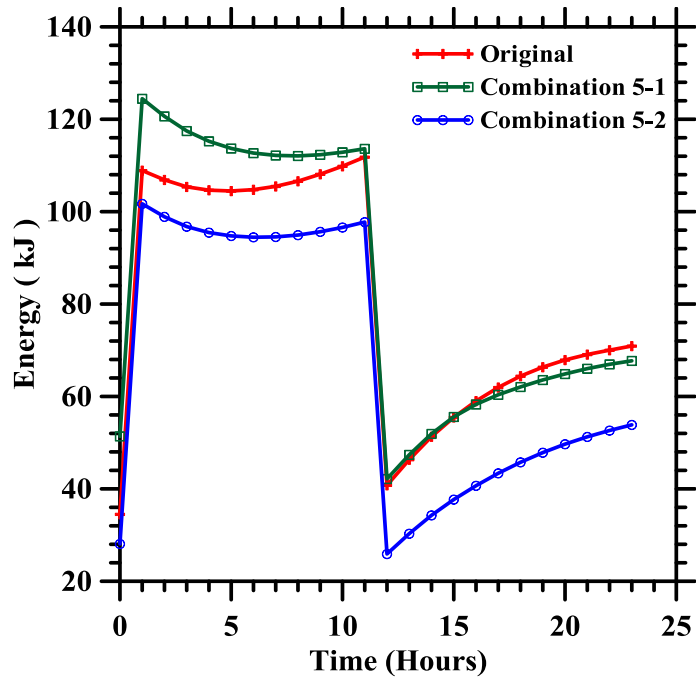
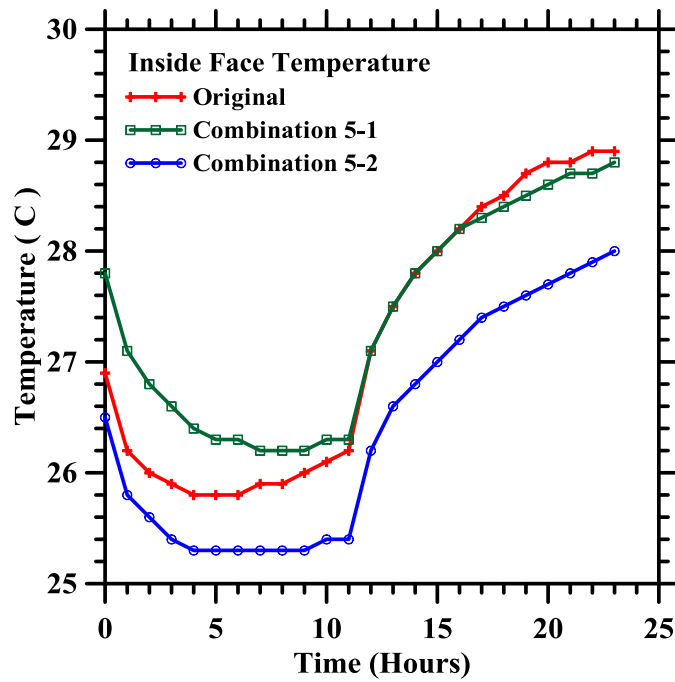


Figure 4-10: Temperature at various locations in the wall and energy flow as a function of time for *Combination 5-2*

The temporal change in EFTIF for *Combinations 5-1* and *5-2* along with that of the *original* case are presented in Figure 4-11(a), which shows the reduced EFTIF for the *Combination 5-2*. The temperature difference between the *original* configuration and *Combination 5-2* varies between 0.1 - 1.0 °C and it is even larger between *Combination 5-1* and *5-2* as seen from Figure 4-11(b). The higher temperatures in the inside face for the *original* and *Combination 5-1* configurations result in higher thermal gradients at the inside face of the wall and hence higher energy flow through the wall.



(a)



(b)

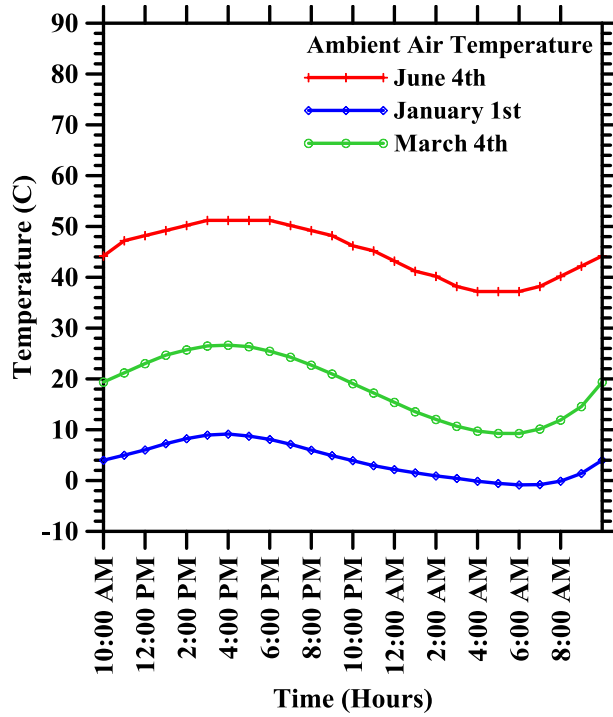
Figure 4-11: Comparison of: (a) energy flow through the inside face (EFTIF), and (b) inside face temperatures for *Combinations 5-1* and *5-2*

5.0 USE OF MULTIPLE PCMS AND GYPSUM WALLBOARDS EMBEDDED WITH PCM

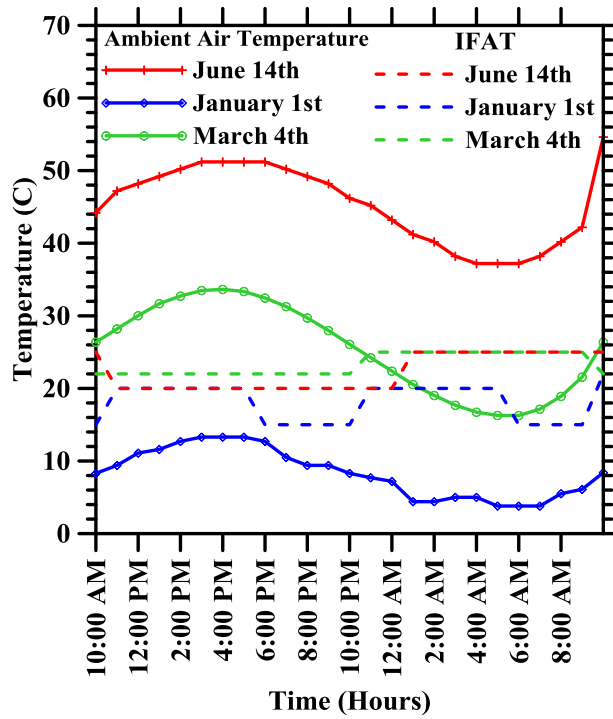
This chapter discusses the incorporation and placement of multiple PCMs in a concrete wall and their effect on output parameters. Also discussed is the incorporation of gypsum wallboards (WB) with varying percentages of PCM D (0% - 30%) placed in a concrete wall and its comparison to a case where pure PCM D is used as a separate layer in equivalent volumes. The typical cyclic behavior of a PCM under extended loading is also investigated.

5.1 Weather Data

The 24 hour variation in the inside face air temperature (IFAT) and ambient temperature can be seen in Figure 5-1. This temperature variation has been used for both the analyses. The equivalent temperature (instead of radiation flux) is calculated as in equation (2.4). This temperature value [43, 51] (Calculation shown in Table 5-1) is added to the actual ambient temperature profile (from Figure 5-1(a)) to obtain the applied ambient temperature profile applied to the wall (shown in Figure 5-1(b)). Here forth in the document, June 14th will be denoted as a hot day, Jan 1st as a cold day and March 4th as a typical day. For comparison between multiple PCM layers weather data from both hot and cold Phoenix days have been used. For analysis of WBs and the equivalent volume of PCM D, weather data from a typical day only is chosen. The exterior convective heat transfer co-efficient, h_e is taken as $20\text{W/m}^2\text{-}^\circ\text{C}$ and the interior convective heat transfer co-efficient, h_{int} is taken as $5\text{W/m}^2\text{-}^\circ\text{C}$.



(a)



(b)

Figure 5-1: Ambient air temperature profile for Phoenix, AZ [43] (a) without radiation (b) with radiation

Table 5-1: Radiation-related Data

Phoenix, Arizona (Day)	Solar Insolation (S)	Absorption Coefficient	he	S* α /he
	W-sec/m ² /sec	(α)	W/ m ² - ⁰ C	⁰ C
June 14 th –Hot day	309.2	0.65	20	10
January 1 st - Cold Day	135.42	0.65	20	4.4
March 4 th - Typical Day	215.42	0.65	20	7

5.2 Materials and Properties

Tomlinson and Heberle [40] developed paraffin impregnated gypsum wallboards, the varying properties of which are listed in Table 5-2. The temperature of phase change of the PCM impregnated in the WB is from 25 - 29 °C and hence the typical day temperature profile is chosen for this analysis. Feustel and Stetiu [53] used the same WB properties to evaluate their latent storage performance. For the study of influence of multiple layers of PCM in a wall, PCM A and PCM C (which were also listed in earlier chapters) are used. Phase change temperature of PCM A is from 27–31 °C; PCM C from 10-14 °C and PCM D from 25-29 °C. Hence the use of PCMs A and C together helps tackle the energy performance during hot and cold days.

The standard wallboard thickness is 1.5cm. The equivalent volume of PCM D that will be used has been calculated with respect to the percentage of PCM in each WB layer and is converted into a change in the PCM D layer thickness (since area of wall remains constant - 1m high x 1m wide) as shown in Table 5-3.

Table 5-2 : Material properties used in the analyses

Material		Density	Specific	Conductivity	Latent
		kg/m ³	kJ/kg-C	W/m-C	kJ/kg
Concrete		2400	0.750	1.450	--
PCM A		800	2.400	0.200	169
PCM C		860	2.000	0.220	185
PCM D		900	2.350	0.250	194
Gypsum Wall board	Conventional (No PCM)	696	1.089	0.173	0
	10% PCM	720	1.215	0.187	19.3
	16% PCM	760	1.299	0.192	31.0
	20% PCM	800	1.341	0.204	38.9
	30% PCM	998	1.467	0.232	58.3

Salyer and Sircar [34] conducted various fire retardation tests on different wallboards and concluded that wallboards with organic PCMs are potentially hazardous and will continue to burn after ignition under normal temperatures. They suggested that limiting the percentage of PCM in wallboards to 20% in order to reduce the hazard.

Table 5-3: Pure PCM D thickness

PCM %	PCM D Thickness (cm)
10	0.15
16	0.24
20	0.3
30	0.45
100	1.5

5.3 Model Details

A concrete wall of height 1m is used, and it is assumed that the heat flow is unidirectional. The temperature of the inside face of the wall, depends on the outside air temperature, the effective thermal resistance of the wall and the temperature maintained by the air-conditioning or heating systems.

In the first set of analysis, the effect on EFTIF of using multiple PCM layers embedded in a 20cm thick concrete wall was studied. In the first case PCM A is placed at 5cm from the outside face of the wall and PCM C is placed at 5cm from the inside face of the wall (here forth mentioned as Case AC-5). In the second case, PCM C is placed at 5cm from the outside face and PCM A is placed at 5cm from the inside face (here forth mentioned as Case CA-5) as shown in Figure 5-2. The results from the 5 layer model are compared to results from 3 layer models (previously discussed). The 3 layer models discussed are Case A-3 and Case C-3; when PCM A is placed in a concrete wall analyzed for a hot day and when PCM C is placed in a concrete wall analyzed for a cold day, respectively.

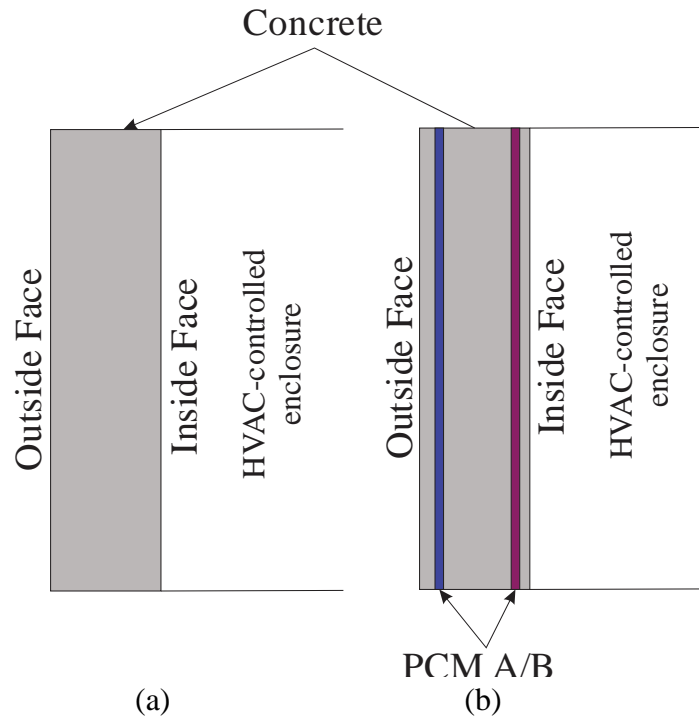


Figure 5-2: (a) Plain concrete wall (b) Both PCMs placed separately (5 Layer Model).

In the second set of analysis a 20cm thick wall has been analyzed using PCM impregnated wallboard (WB) of thickness 1.5cm, placed on the inside face of the concrete wall (see Figure 5-3). This analysis is run over a one week period where the ambient air temperature for any typical day of the week varies as shown in Figure 5-1. The efficiency of WBs is compared to an equivalent volume of PCM embedded as a single layer placed at the inside face of the wall. The amount of PCM percentage in the WB varies from 0%, 10%, 16%, 20% and 30% in the wallboards. An additional 1.5cm thick PCM D layer (100% by volume of WB) is also analyzed.

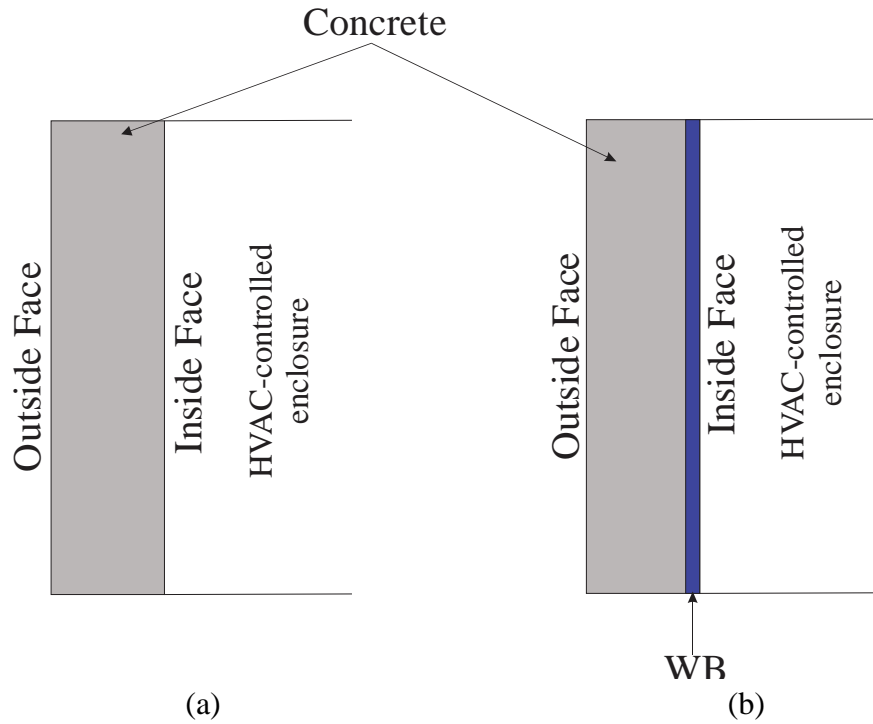


Figure 5-3: (a) Plain concrete wall (b) Concrete wall with centrally placed gypsum WB

It is assumed that the inside air is maintained within a temperature of 15-20 °C on a cold day and 20-25 °C on a hot and typical day (for Phoenix, Arizona). Other assumptions made for these analyses are: all the layers are homogenous and isotropic, thermal properties of concrete and PCM are constant, thermal expansion of concrete and PCM is negligible, natural convection effect inside the liquid PCM is ignored, all surfaces other than the outside and inside surfaces are insulated and no heat flow occurs in the y and z direction, i.e. heat flow is one-dimensional.

5.4 Numerical Results

Section 5.4.1, presents the use of multiple PCM layers in various placement combinations. In section 5.4.2, comparison is made between varying percentages (by volume) of PCM embedded in a 1.5cm thick gypsum board where the WB is placed at the inside face of the wall.

5.4.1 Use of Both PCM A and PCM C Together

In this section, two cases are discussed - when PCM A and PCM C are placed in the wall simultaneously so as to account for both hot and cold days in Phoenix, AZ. In both the cases, AC-5 and CA-5, the thickness of each individual PCM layer (PCM A and PCM C) is 50% of total PCM thickness. Only the total PCM thickness is referred to in the coming sections, instead of referring to individual PCM thicknesses. For cases A-3 and C-3 that are used for comparison, the thickness of PCM for the 3 layer model is same as thickness of both PCMs together in the 5 layer model. In the case for cold days it was observed that EFTIF and temperature of inside face of the wall stabilize after 7 days so results for only the 7th day have been discussed for this case.

Temperature variation across wall

As can be seen from Figure 5-4 and Figure 5-5, the temperature of the inside face decreases with increase in PCM thickness for hot weather and increases with increasing PCM thickness for cold weather conditions which is the expected result, although the difference is most prominent during hot weather than during the cold weather. This is likely because of the fact that the ambient conditions for the hot weather day are much larger than the phase change

temperature of the PCM used to account for higher temperatures (PCM A) whereas the PCM D has a phase change temperature range much closer to the ambient conditions of a cold weather day. Position of the two PCMs with respect to each other (Case AC-5 and CA-5), does not affect the temperature on the inside face of the wall.

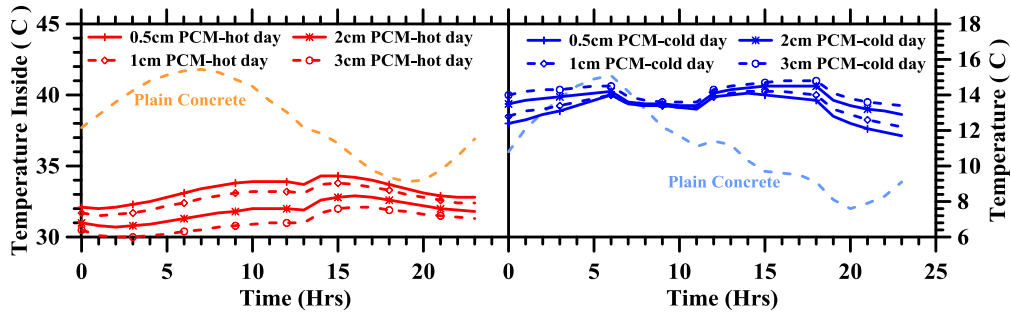


Figure 5-4: Temperature of the inside face for Case AC-5

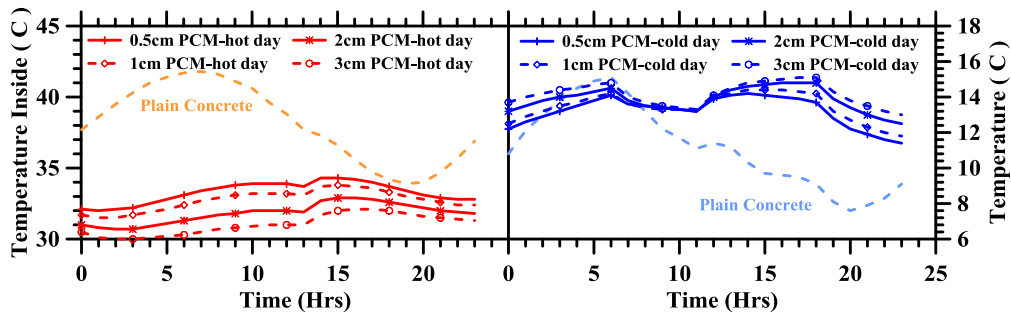


Figure 5-5: Temperature of the inside face for Case CA-5

Energy stored in PCM

Figure 5-6 shows the energy stored by both PCM A and PCM C for the two different cases discussed. Since PCM A is suitable for a hot day and PCM C is suitable for a cold day, PCM A does not store any latent heat on a cold day and PCM C does not store any latent heat on a hot day. For a hot day the latent energy stored does not change for PCM A after the first few hours i.e. it reaches

maximum latent heat capacity, and hence the efficiency remains 100% at all times irrespective of its position within the wall. PCM C stores a maximum energy of 52% of its total capacity when placed near the outside; but it stores about 78% of its total capacity when placed near the inside. Further investigations showed that only part of the PCM C layer is within its phase change temperature range in cases CA-5 and C-3 but in case AC-5 the entire layer is within the phase change temperature range at all times. Hence, PCM C stores highest amount of latent energy in case AC-5.

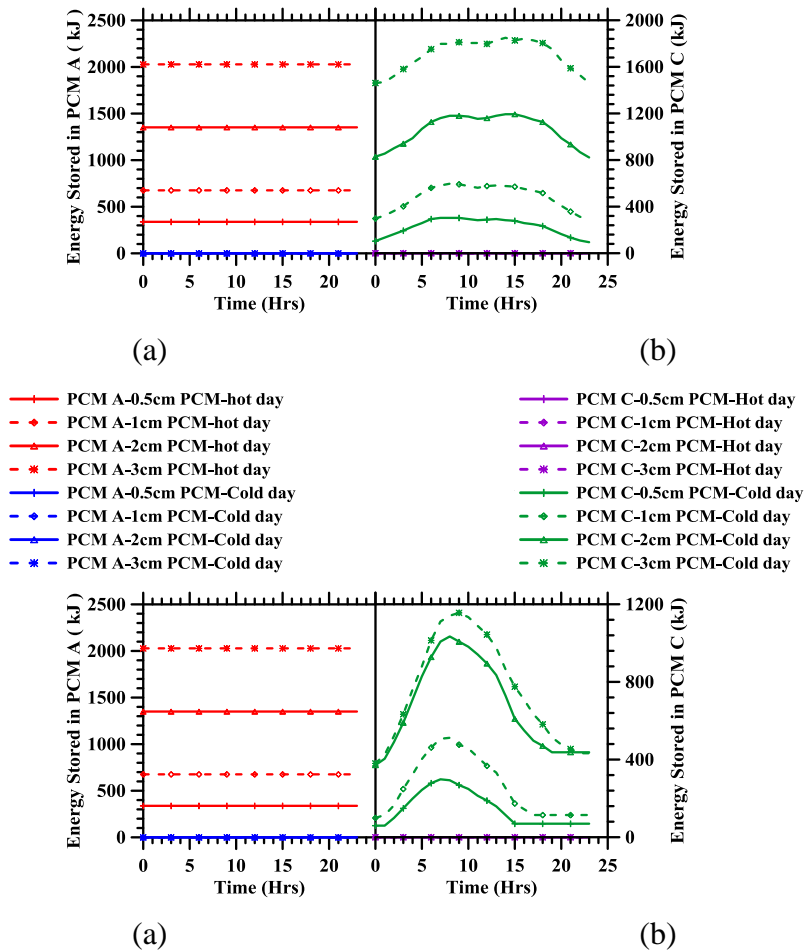


Figure 5-6: Cumulative latent energy stored in (a) PCM A and (b) PCM C for Case AC-5; and in c) PCM A and (d) PCM C for Case CA-5

Energy flow into and out of the room

Figure 5-7 shows EFTIF variation over time for both cases. It is seen that increase in PCM thickness reduces EFTIF. Also, placement of either PCM with respect to the other does not affect EFTIF. Each graph shows two zones corresponding to daylight hours when energy demand to cool the inside air is high and nighttime when energy demand is relatively lower. The drop in EFTIF values after 12 hours can be attributed to the increase in the IFAT values at night. Since, the difference between the ambient and IFAT temperatures is lesser at night, the work done by the wall/PCM is lesser and hence lower EFTIF values are seen. Lower values of EFTIF are seen in walls with PCM than in a pure concrete wall as expected. An EFTIF decrease of up to 200 kJ (51%) can be obtained by adding PCM for hot days and a decrease of up to 90 kJ (54%) for cold days.

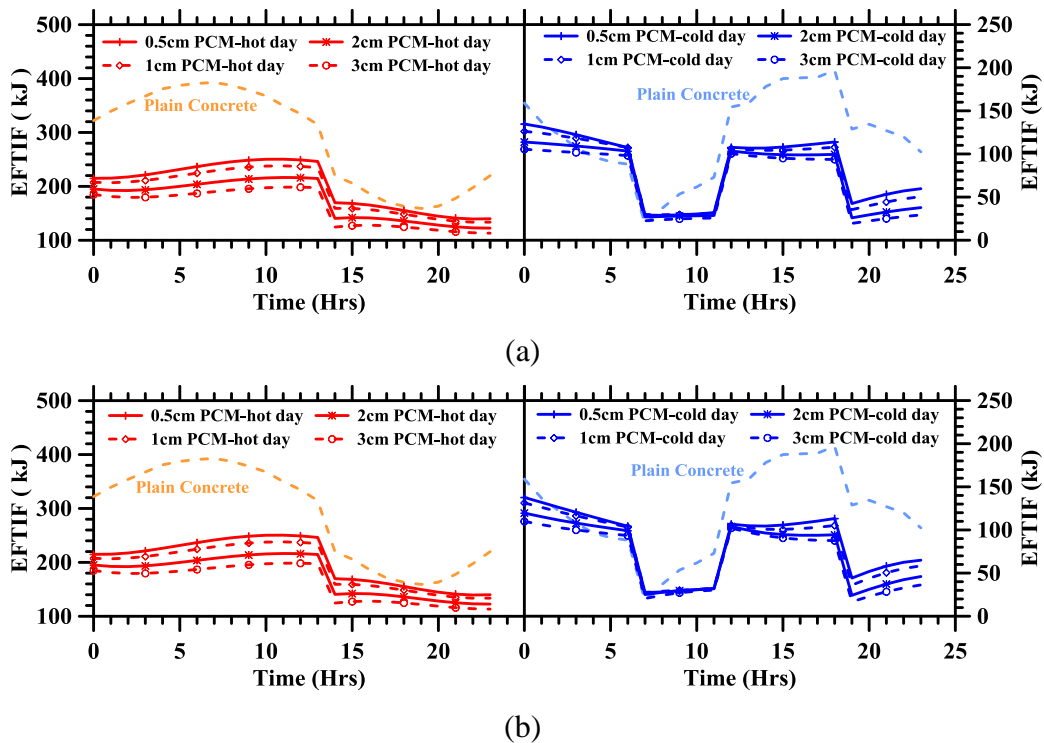


Figure 5-7: EFTIF (a) for Case AC-C; (b) for Case CA-C

Table 5-4 and Table 5-5 show EFTIF and savings over a 24 hour period. Energy savings increases as total PCM thickness increases, as expected. This shows that the placement of each PCM relative to each other does not affect the EFTIF values, and neither does placing both PCMs together or apart affect the EFTIF values. Therefore, the EFTIF values are a function of PCM thickness and material properties only.

Table 5-4: EFTIF and Energy savings for a Hot Day

Hot day - 14th June				
PCM thickness	CA-5		AC-5	
	Separate		Separate	
	EFTIF	Savings	EFTIF	Savings
	kJ	%	kJ	%
0	6932		6932	
0.5	4829	30.3	4829	30.3
1	4599	33.6	4600	33.6
2	4200	39.4	4200	39.4
3	3864	44.3	3864	44.3

As seen in Table 5-4, for a hot day, energy savings in the 5 layer model is slightly less than that of the wall with only PCM A of the same thickness irrespective of position. This is an expected result since in a 5 layer model the thickness of PCM A only is half as that in a 3 layer model, which means the energy storage capacity also becomes half of that of a 3 layer wall. In this case contribution from PCM C is neglected since it does not store any latent heat.

Table 5-5 shows results for a cold day when PCM C is active and PCM A is mostly redundant. In this case, slightly different results are seen, the energy savings of a 5 layer model are higher than that of a 3 layer model. To explain the results better, only a 3cm PCM layer model is chosen for each case, which is discussed in detail.

Table 5-5: EFTIF and Energy savings for a Cold Day

Cold day - 1st Jan				
PCM thickness	CA-5		AC-5	
	Separate		Separate	
	EFTIF	Savings	EFTIF	Savings
	kJ	%	kJ	%
0	2911		2911	
0.5	2028	30.3	2028	30.3
1	1931	33.7	1931	33.6
2	1763	39.4	1764	39.4
3	1622	44.3	1625	44.2

Discussion for a 3cm thick PCM Layer

Figure 5-8 shows energy flow at different points across the wall thickness for Cases CA-5 and AC-5. The total energy flowing into and out of the wall at the outside face is higher for case CA-5 than for case AC-5. The layer of PCM C when placed near the outside retards the flow of energy across itself. This is effect is not seen when the PCM A layer is placed near the outside for a cold day.

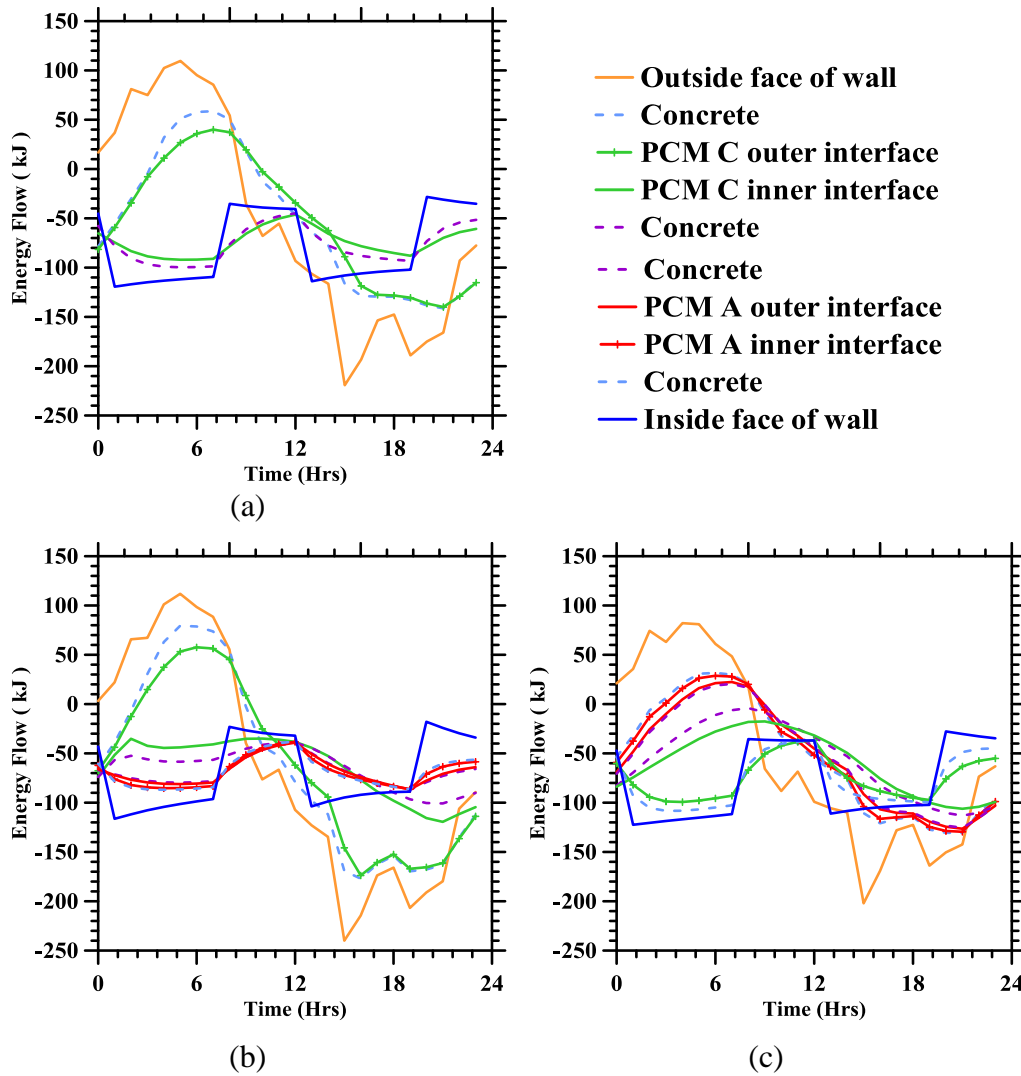


Figure 5-8: Energy flow at different points across wall thickness (a) Case C-3
(b) Case CA-5 (c) Case AC-5

These results can be attributed to the placement of PCM C within the concrete layer. When any PCM is placed closer to the inside face of the wall it will tend to affect the EFTIF more than when compared to PCMs placed near the outside face because the parameter of interest is the energy flow through the inside face. The thermal conductivity of PCM A is lower than that of PCM C and the specific heat capacity of PCM A is higher than that of PCM C. PCM A acts as

a thermal barrier letting in lesser heat to the PCM C layer in the CA-5 case. Hence, case CA-5 shows lower EFTIF values.

Energy savings in almost all the cases considered are not significantly different. Thus it can be concluded that the placement location of PCM does not influence EFTIF significantly. A slightly better case would be when the PCM with a higher phase change temperature is placed near the inside face and the PCM with lower phase change temperature is placed near the outside face (Case CA-5). In any case, even if a 3 layer model might be better suited for a particular day, to account for all possible weather models, a multiple PCM layer wall model with two PCMs placed together should be considered.

In other words PCMs can be placed in any order at any location within the concrete wall as feasible for construction. In the previous chapter, the effect of placement a single PCM layer on the outside and inside faces of a concrete wall was evaluated and similar conclusions obtained. Combining both results we can say that placement of PCMs at any location from outside face of the wall to the inside face would not affect EFTIF in any way. In such cases precedence should be given to construction constraints.

5.4.2 Comparison between WB and Pure PCM D

Temperature variation across wall

Figure 5-9 shows variation of temperature at the inside face of the wall with respect to time. Using a 1.5cm pure PCM D layer shows lower inside face temperatures than using WBs, which in turn shows lower inside face temperatures than using pure PCM D layers of same volume. At nighttime, concrete wall with a 1.5cm PCM D layer shows higher inside temperatures than WB's which in turn show higher inside temperatures than equivalent volumes of PCM D and vice versa during daytime.

It can be clearly seen that although the peak ambient air temperature is reached after 6 hours (refer Figure 5-1), the peak temperature at the inside face of the wall is reached after 12 hours in case of a plain concrete wall, after 12-15 hours when WB is placed in the wall, after 12-13 hours for equivalent PCM D volume and after 14-17 hours when a 1.5cm PCM D layer is used. This shows that the time lag for the temperature inside to rise above the IFAT temperature range is higher for wall with 1.5cm PCM D layer than for WB than for equivalent volumes of pure PCM. For a WB embedded with 30% paraffins, cost data was taken from [54]. Cost of wallboards embedded with PCM is \$6.35/kg and cost of pure PCM is \$4.41/kg. Therefore, using a 1.5cm PCM D layer would be the best case for energy conservation, and would be less expensive than using WBs, provided the embedment of pure PCM layer can be satisfactorily accomplished. This analysis does not consider any other structural effects that might favor the use of a wallboard.

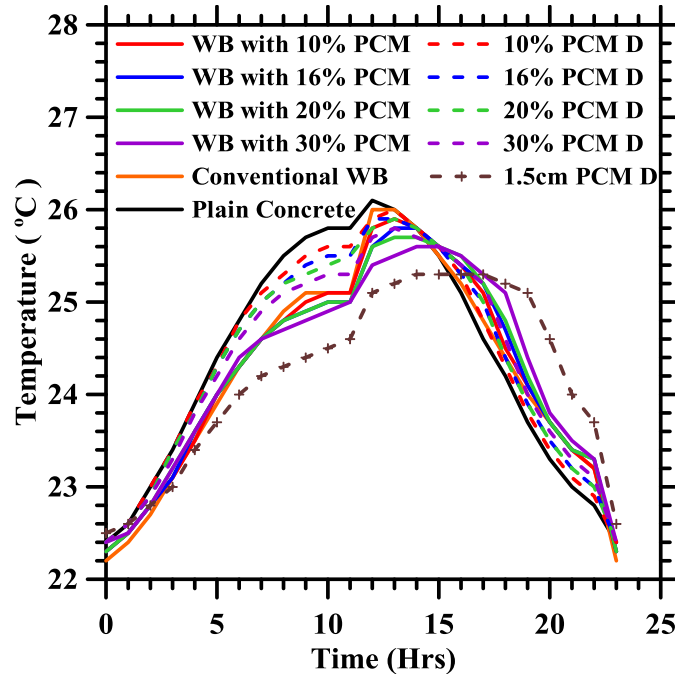


Figure 5-9: Temperature variation inside the room with respect to time

Energy flow into and out of the room

Figure 5-10 (a) shows EFTIF when WBs and equivalent PCM are used with respect to % of PCM present. 0 on the % of PCM scale denotes a both plain concrete wall and conventional (0% PCM) WB. Use of 1.5cm layer of PCM D in a concrete wall shows a lower value of EFTIF than that obtained by use WBs, which in turn shows lower EFTIF than that for an equivalent volume of pure PCMs (0-30% PCM). This means that EFTIF decreases and savings increase as the percentage of PCM increases (refer Table 5-6).

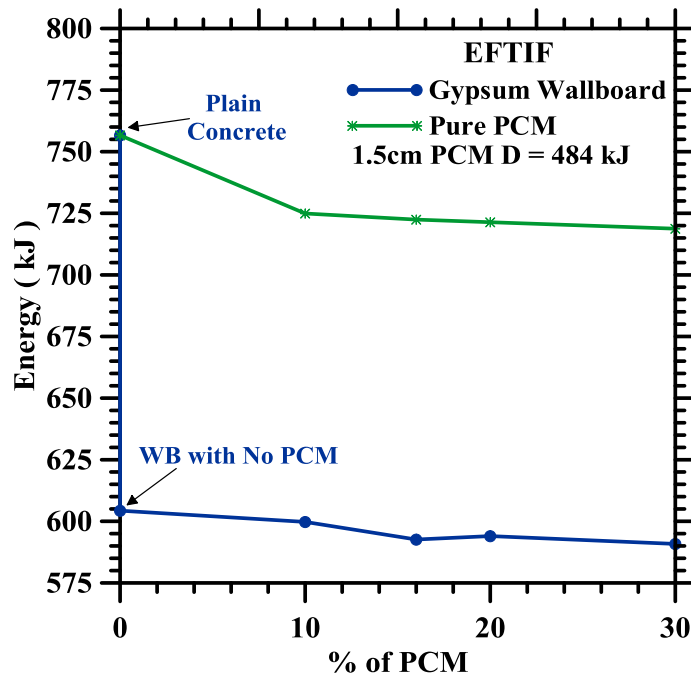
Figure 5-10 (b) shows variation of EFTIF over the second 24 hour period. The two different zones in the graph correspond to daytime and nighttime respectively. Higher energy flow is required to cool the inside during the day and lower energy flow is required to heat the inside at night. Highest ambient air

temperature on a typical day is seen after 6 hours and lowest temperature is seen after 19 hours. The maximum EFTIF during the daytime is seen after 9-11 hours (with a lag of 4 hours) for a concrete wall with WBs and pure PCMs.

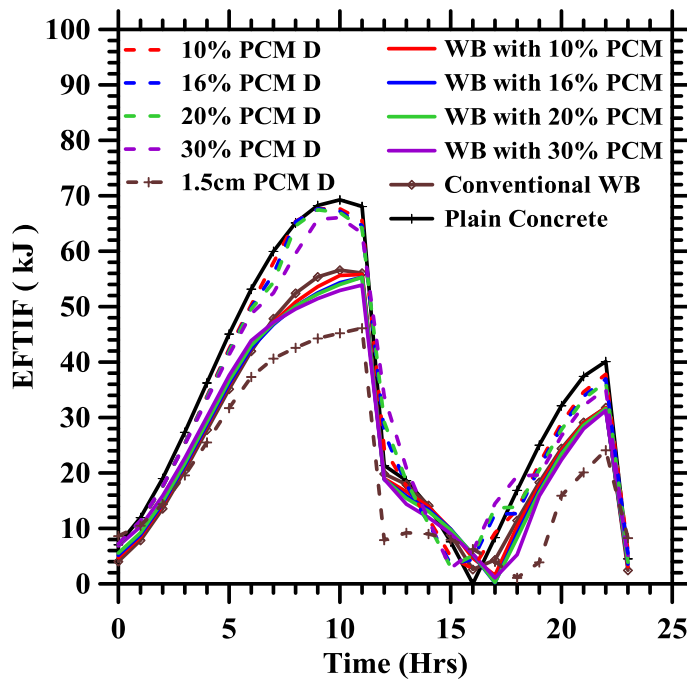
At nighttime close to zero EFTIF values are seen for all cases (viz. at 15-17 hours for all cases), except for a 1.5cm layer of PCM D, where the lower EFTIF is seen after 18 hours and 12 hours. If we refer to Figure 5-9, it is seen that the temperature of the inside face of the wall approaches 25 °C (IFAT) at almost the same time as the EFTIF reaches zero. Since, the wall temperature reaches the IFAT temperature, no more energy is consumed. In the case of a 1.5cm layer PCM D, EFTIF reaches 0 at two points (viz. 12 and 18 hours) because the inside temperature remains almost constant at 25 °C within this time period. Again this shows that the best case scenario would be using a 1.5cm pure PCM D layer.

Table 5-6: EFTIF data summary for section 4.2

% of PCM	PCM embedded WB		Equivalent volume of Pure PCM D	
	EFTIF (kJ)	Savings (%)	EFTIF (kJ)	Savings (%)
Plain Concrete	757		757	
Wallboard (No PCM)	604	20.1	N/A	N/A
10% PCM	600	20.7	725	4.2
16% PCM	593	21.7	722	4.5
20% PCM	594	21.5	721	4.7
30% PCM	591	21.9	719	5.0
1.5 cm Pure PCM	-	-	484	36.0



(a)



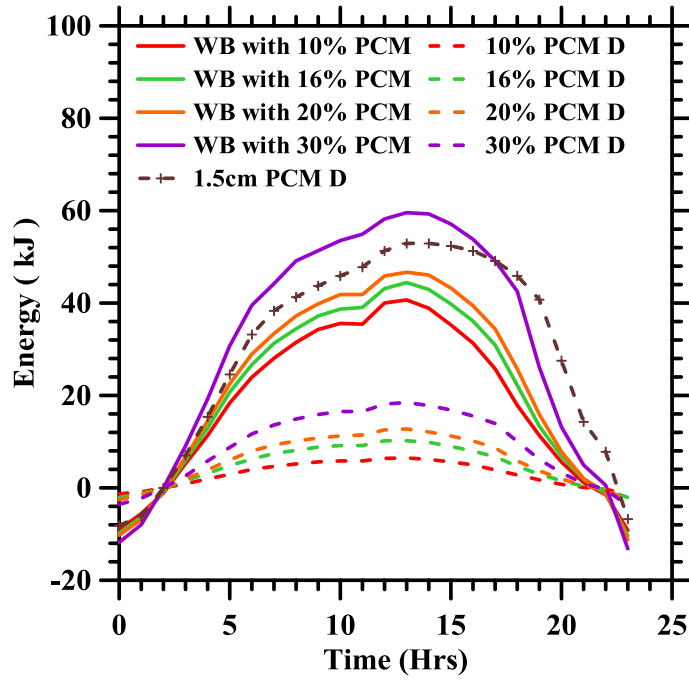
(b)

Figure 5-10: (a) Energy flow into and out of the room with respect to thickness

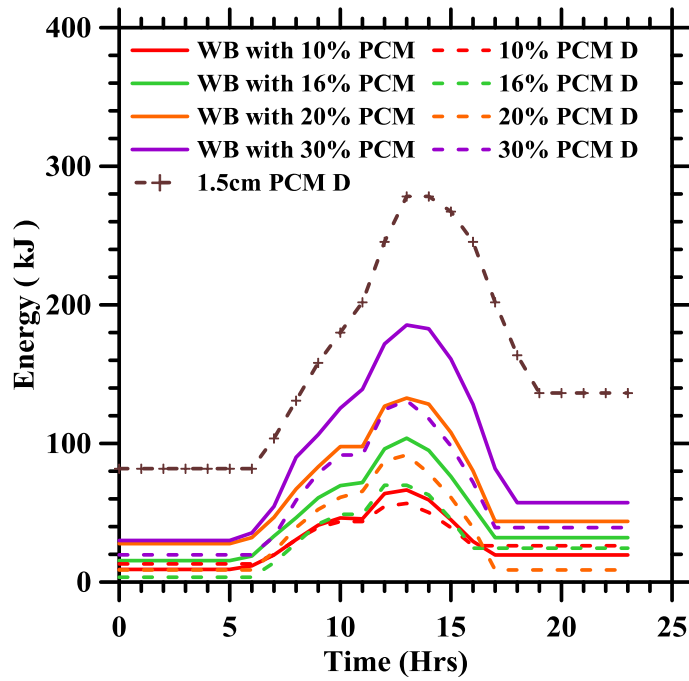
(b) Energy flow into and out of the with respect to time

Energy stored in PCM

Figure 5-11 shows cumulative sensible and latent energy stored by PCM as a function of time. Increasing portion of the curve (during the day) indicates energy storage by PCM and the decreasing portion (at nighttime) indicates energy released by PCM to the inside. Latent energy is stored/released by the PCM only during peak hours of the day (i.e. between 3rd to 17th hours) when the temperature of the PCM reaches its phase change temperature. Hence, a change in the curve is observed. During the rest of the day (i.e. 0-3 hours and 17-24 hours) there is no change in the total latent energy stored in the PCM. The increment seen during the 0th hour is the net latent energy stored during the first 48 hours. The temperature of the PCM/WB layer is always within the phase change temperature range, but when pure PCM D is used in equivalent volumes the difference in temperature (ΔT) at any given time is always less than for the case when WBs embedded with PCMs are used. Since, magnitude of latent heat stored/released depends on ΔT at any given point, pure PCM layers absorb less latent energy compared to PCM embedded WBs at any given time. A PCM layer of 1.5cm stores higher amount of energy as compared to all the other cases.



(a)



(b)

Figure 5-11: (a) Sensible energy (b) Latent energy; stored in PCM with respect to time

Cyclic Nature over long periods

A typical day ambient temperature is perfectly cyclic and varies above and below the phase change temperature of PCM D impeccably. Hence, these particular results have been used to show the cyclic nature of temperature and energy profiles. As can be seen from Figure 5-12, temperature of inside face, EFTIF and cumulative sensible energy stored (results not reported) have a repeating pattern after the first 24 hours which discounts the effect of all initial conditions on the analysis. The slight irregularity at every 12-13 hours in the EFTIF graphs signifies the transition period where the ambient temperature falls below the IFAT temperature (Figure 5-1). In the EFTIF curve (Figure 5-12(b)) the irregularities at every 24-26 hours correspond to the period where ambient temperature rises above the IFAT temperature. Since, heat flow is hindered by the action of PCM, the inside temperature curve is relatively more smooth.

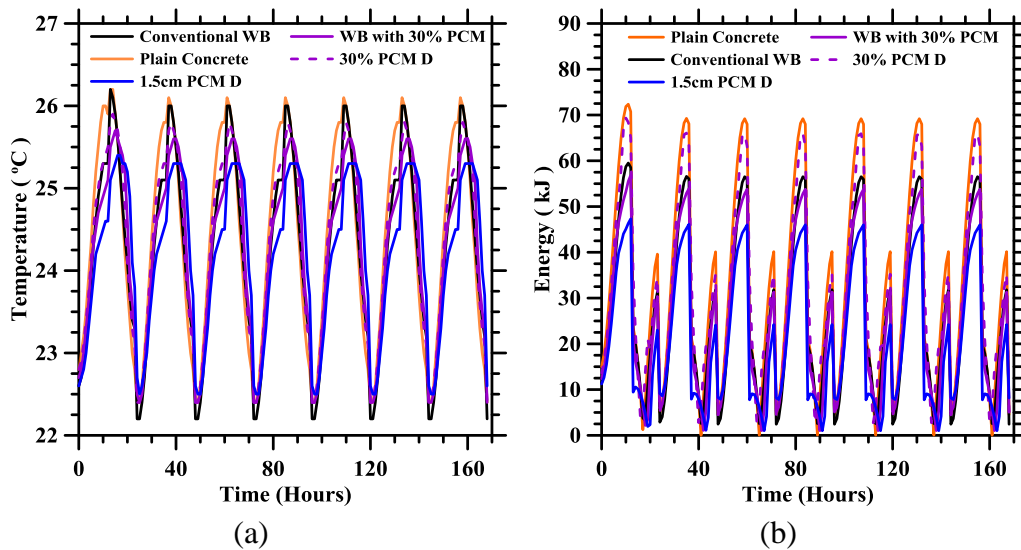


Figure 5-12: Temperature of inside face (a) EFTIF with respect to time over one week

The only exception to the general rule appears to be the cumulative latent heats stored by the PCM shown in Figure 5-14. Latent heat stored in a day is higher than that released. Hence, the latent heat storage though cyclic, shows increments at every time step. The latent energy stored every 24 hours is the same after the first 24 hours (Figure 5-13(a)), which can be attributed to the initial conditions of the analysis. Hence, to negate this effect completely, results from only the second day have been discussed throughout the study.

If the analysis is carried out for a longer period, after the PCM reaches its maximum storage capacity, the latent energy storage curve becomes perfectly periodic for all cases as seen in Figure 5-14. The time when the latent heat stored by PCM becomes perfectly periodic depends on the PCM mass, PCM thickness and method of PCM incorporation.

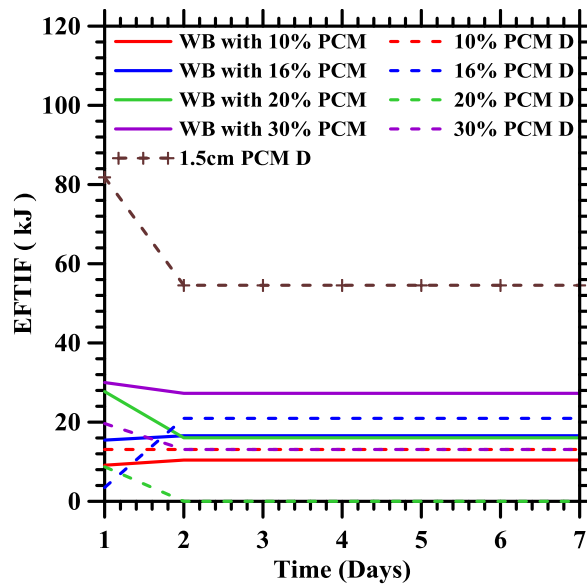
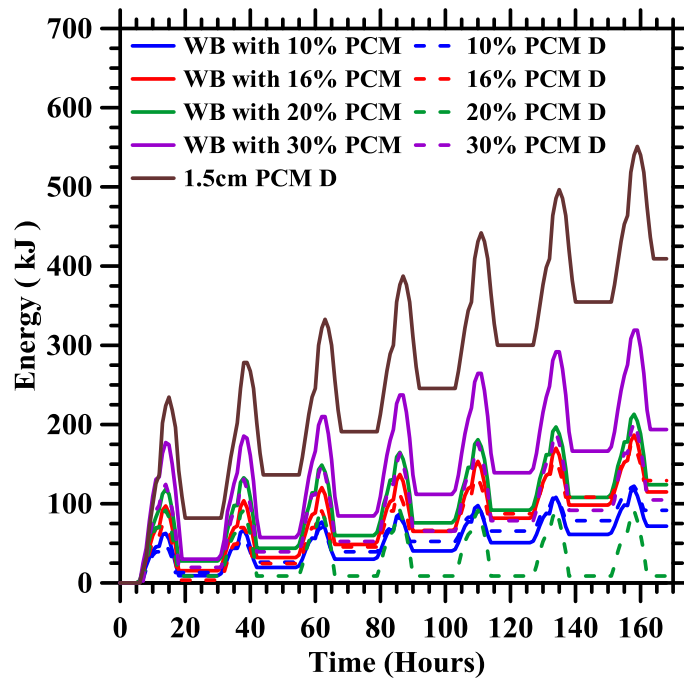
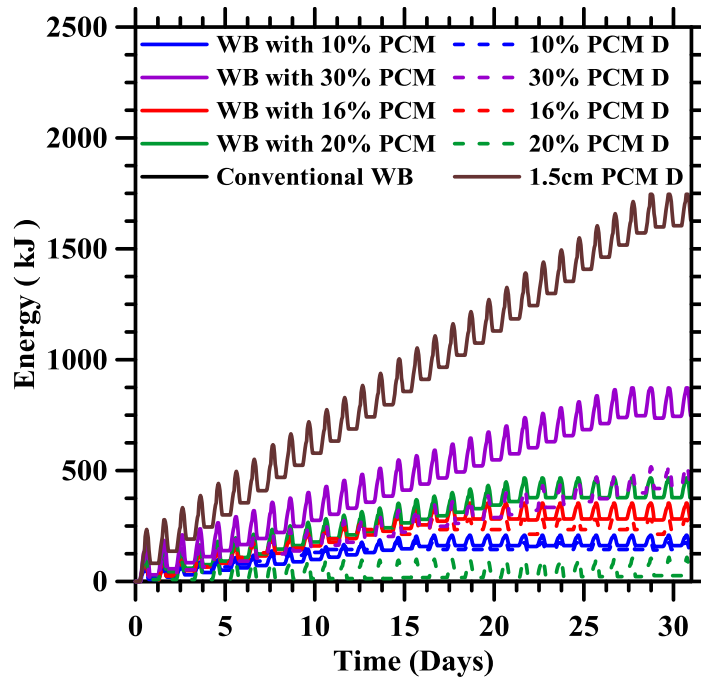


Figure 5-13: Net latent energy stored in PCM each day



(a)



(b)

Figure 5-14: Latent energy stored in PCM with respect to time over

6.0 CONCLUSIONS & FUTURE WORK

6.1 Conclusions

A framework for studying the performance of thermal efficiency of external walls in buildings made using Portland cement concrete is developed in this paper. This framework allows for studying the effects of several structural and material design parameters commonly used in building analysis and designs - wall thickness, type of concrete, PCM type, thickness and location, and external and internal temperature profiles. By changing the material parameters, the design can be implemented for a variety of material types, subjected to wide ranging climatic conditions. Since multiple weather scenarios are considered in this study, the framework can be readily extended to include other desirable scenarios, so that a comprehensive solution for all seasonal weather patterns using multiple PCM types and layers can be developed. Further analysis to include the effects of using wallboards and multiple PCMs in buildings and changing wall thickness to better understand thermal efficiency needs are provided. The process is automated, aiding in increased processing speed. The computational framework requires very little computer memory and wall clock time (about 80 s for a 48 hour simulation on a Pentium 4-E5440-2.83 GHz Workstation running Windows 7) to obtain the response and hence can be used effectively in finding optimal solutions where hundreds of analyses are usually required.

The major findings from this study are summarized below:

Effect of varying PCM thickness and location:

- i. The use of PCMs as a layer in the concrete wall helps the regulation of inside temperature. For the cases studied in this paper, larger PCM layers are beneficial for hotter temperatures where the latent heat capacity of the PCM is better utilized. Also, the increased thermal resistance and specific heat of lightweight concrete is found to provide a better thermal barrier compared to normal weight concrete. PCM incorporated lightweight concrete wall design is generally found to be a better methodology to reduce HVAC costs in hot climates. However this conclusion is not applicable when the PCM layer thickness is very large, in which case the wall type becomes inconsequential in the energy performance.
- ii. Temperature of inside face decreases with increasing PCM thickness when ambient temperature is higher than IFAT and increases with increasing PCM thickness when ambient temperature is lower than IFAT. EFTIF decreases and savings increase with increase in PCM mass for any model including PCMs.
- iii. The energy flow into the building decreases almost linearly with increasing PCM thickness for both the normal weight and lightweight concrete walls. For a 5 cm thick PCM layer in the wall, the EFTIF values are only about 40% as that of the baseline case for both normal and lightweight concrete.
- iv. For the two geographic locations considered in this study and the boundary conditions, the overall thermal response is relatively insensitive to the

location of the PCM layer. Numerical results show a slightly better response for PCM placed closer to the inside face of the wall compared to other locations, especially for hotter climates.

- v. A set of optimal PCM properties for the desired ambient impulse can be obtained using the simulations described in this study. The ad-hoc procedure reported here works for a small number of design parameters. However, a formal design optimization framework (using formal nonlinear programming techniques such as gradient-based and population-based methods) will make it possible to find the best possible combination of the PCM and wall design parameters and allow for the inclusion of life-cycle analysis in the design process.

Use of multiple PCMs and gypsum wallboards:

- vi. Effect of initial conditions can be seen during the first day of any analysis. Stable results/Perfectly periodic results can be seen only after the second day. Except for latent heat stored in PCM all other factors (EFTIF, inside temperature, sensible energy stored etc) are perfectly periodic after the first 48 hours. Latent heat storage curve becomes perfectly periodic after PCM reaches its storage capacity. The only case where results stabilize after 7 days is when a cold day PCM is introduced into the model.
- vii. When using multiple PCMs in a concrete wall, neither use of single or multiple PCMs nor placement of the PCM affects output parameters studied. Hence precedence could be given to construction feasibility and artistic wishes.

- viii. WBs show lower inside temp than concrete walls with pure PCM of equivalent volume, since lag for heat reaching inside face of wall is higher for wall with PCMs and PCM embedded WBs than for pure concrete wall. At nighttime for the given combination EFTIF touches 0, since inside temperatures reach the IFAT temperatures.
- ix. More savings is seen in case of WBs than in case of pure PCM of equivalent amount. Highest savings is obtained for the case of 1.5cm pure PCM. Since, cost of PCMs is less than that of PCM incorporated WBs, preference should be given to use of pure PCM layers than WBs.

6.2 Future Work

Current research work deals with PCMs and their applications in sustainable construction. The framework developed is preliminary and deals with specific cases. This framework can be advanced further for optimization of wall design (material properties, thicknesses) to minimize the lifetime costs. Minimization of energy consumption and material/maintenance costs are two very important considerations. The framework can also be further modified to include discontinuities in the geometry of the wall model like to include openings. Furthermore non-linear finite element analysis can be included into the framework to eliminate dependence on ABAQUS or any other FEA software. Moreover structural analysis needs to be done on selected wall segments to improve strength of the wall with PCM.

REFERENCES

- [1] Federal Research and Development Agenda for Net Zero Energy, High Performance Green Buildings, National Science and Technology Council (NSTC) (2008) 60
- [2] Buildings Energy Data Book, <http://buildingsdatabook.eren.doe.gov> (accessed on June 2012)
- [3] F. Kuznik, D. David, K. Johannes and J. J. Roux, A review of PCM integrated in building walls, *Renewable and Sustainable Energy Reviews* 15 (1) (2011) 379-391
- [4] H. Mehling and L. F. Cabeza, *Heat and cold storage with PCM*, Springer-Verlag, Berlin (2008).
- [5] F. Demirbas, Thermal energy storage and phase change materials: an overview. *Energy Sources, Part B: Econ Plann Policy* 1 (2006) 85-95.
- [6] V.S.A. Padmaraju, M. Vignesh and N. Nallusamy, Comparative study of sensible and latent heat storage systems integrated with solar water heating unit, International conference on Renewable Energy and Power Quality, Santander, Spain (2008).
- [7] R. Kelly, AMEC Design, Latent heat storage in building materials (2000).
- [8] D. Zhou, C.Y. Zhao and Y. Tian, Review on thermal energy storage with phase change materials (PCMs) in building applications, *Applied Energy* 92 (2012) 593-605
- [9] L.F. Cabeza, A. Castell, C. Barreneche, A. de Gracia and A.I. Fernandez Materials used as PCM in thermal energy storage in buildings: A review, *Renewable and Sustainable Energy Reviews* 15 (3) (2010) 1675-1695.
- [10] S. B. Sadineni, S. Madala, R. F. Boehm , Passive building energy savings: A review of building envelope components, *Renewable and Sustainable Energy Reviews* 15 (8) (2011) 3617-3631
- [11] V. V. Tyagi, D. Buddhi , PCM thermal storage in buildings: A state of art, *Renewable and Sustainable Energy Reviews* 11(6) (2007) 1146-1166
- [12] Y. Zhang, G. Zhou, K. Lin, Q. Zhang, H. Di, Application of latent heat thermal energy storage in buildings: State-of-the-art and outlook, *Building and Environment* 42 (6) (2007) 2197-2209

- [13] N. Neithalath, G. Sant, Phase change materials in concrete: A new strategy to improve the thermal damage resistance and thermal energy efficiency of concrete structures, (unpublished results)
- [14] A. Sharma, V.V. Tyagi, C.R. Chen, D. Buddhi, Review on thermal energy storage with phase change materials and applications *Renewable and Sustainable Energy Reviews*, 13 (2) (2009) 318-345
- [15] D. Zhang, J. Zhou, K. Wu, Z. Li, Granular phase change composites for thermal energy storage, *Solar Energy* 78 (3) (2005) 471–480.
- [16] M. Kenisarin and K. Mahkamov, Solar energy storage using phase change materials, *Renewable and Sustainable Energy Reviews*, 11(9) (2009) 1913-1965
- [17] C.K. Halford and R.F. Boehm, Modeling of phase change material peak load shifting, *Energy and Buildings*, 39(3) (2007) 298-305
- [18] B.M. Diaconu and M. Cruceru, Novel concept of composite phase change material wall system for year-round thermal energy savings, *Energy and buildings*, 42 (10) (2010) 1759-1772
- [19] A. Vaz Sa, M. Azenha, H. de. Sousa and A. Samagaio, Thermal enhancement of plastering mortars with Phase Change Materials: Experimental and numerical approach, *Energy and Buildings*, 49 (2012) 16-27.
- [20] A.M. Khudhair and M.M. Farid, A review on energy conservation in building applications with thermal storage by latent heat using phase change materials, *Energy Conversion and Management*, 45(2) (2004) 263-275.
- [21] A.L.S. Chan, Energy and environmental performance of building façades integrated with phase change material in subtropical Hong Kong, *Energy and Buildings*, Volume 43, Issue 10, October 2011, Pages 2947-2955
- [22] D. Zhang, Z. Li, J. Zhou, K. Wu, Development of thermal energy storage concrete, *Cement and concrete research*, 34(6) (2004) 927-934
- [23] A. Pasupathy, L. Athanasius, R. Velraj and R.V. Seeniraj, Experimental Investigation and numerical simulation analysis on the thermal performance of a building roof incorporating phase change material (PCM) for thermal management, *Applied Thermal Engineering* 28 (5–6) (2008) 556-565
- [24] F. Kuznik, J. Virgone, and J. Noel, Optimization of a phase change material wallboard for building use, *Applied Thermal Engineering*, 28(11-12) (2008) 1291-1298
- [25] H. Zhang, Q. Xu, Z. Zhao, J. Zhang, Y. Sun, L. Sun, F. Xu, Y. Sawada, Preparation and thermal performance of gypsum boards incorporated with

microencapsulated phase change materials for thermal regulation, *Solar Energy Materials and Solar Cells* 102 (2012) 93-102

[26] S.G. Manari, Thermal response of cementitious systems incorporating phase change materials, M.S Thesis, Clarkson University (2011) 106.

[27] L. Zalewski, A. Joulin, S. Lasseu, Y. Dutil and D. Rouse, Experimental study of small-scale solar wall integrating phase change material, *Solar Energy* 86(1) (2012) 208-219.

[28] F. Berroug, E.K. Lakhal, M. El. Omari, M. Faraji and H. El. Qarnia Thermal performance of a greenhouse with a phase change material north wall, *Energy and Buildings* 43(11) (2011) 3027-3035.

[29] E. Rodriguez-Ubinas, L. Ruiz-Valero, S. Vega J. and Neila, Applications of Phase Change Material in highly energy-efficient houses, *Energy and Buildings* 50 (2012) 49-62

[30] A. Carbonari, M. De Grassi, C. Di Perna and P. Principi, Numerical and experimental analyses of PCM containing sandwich panels for prefabricated walls, *Energy and Buildings* 38(5) (2006) 472-483.

[31] C. Zhang, Y. Chen, L. Wu and M. Shi, Thermal response of brick wall filled with phase change materials (PCM) under fluctuating outdoor temperatures, *Energy and Buildings* 43(12) (2011) 3514-3520

[32] M.J. Huang, P.C. Eames and N.J. Hewitt, The application of a validated numerical model to predict the energy conservation potential of using phase change materials in the fabric of a building, *Solar Energy Materials and Solar Cells* 90(13) (2006) 1951-1960

[33] K. Darkwa and P.W. O'Callaghan, Simulation of phase change drywalls in a passive solar building, *Applied Thermal Engineering* 26(8-9) (2006) 853-858

[34] I.O. Salyer and A.K.Sircar, Phase change materials for heating and cooling of residential buildings and other applications, *Proceedings of the 25th Intersociety Energy Conversion, Engineering Conference, Reno, NV* (1990).

[35] I.O. Salyer and A.K.Sircar, Development of phase change technology for heating and cooling of residential buildings and other applications, *Proceedings of Intersociety Energy Conversion Engineering Conference*, 28 (2) (1993) 133-142.

[36] M. Ahmad, A. Bontemps, H. Sallee and D. Quenard, Experimental investigation and computer simulation of thermal behaviour of wallboards containing a phase change material, *Energy and Buildings*, 38 (2006) 357-366.

- [37] A. Rudd, Phase-Change Material Wallboard for Distributed Thermal Storage in Buildings, s.l. : Building Science Press, 1993.
- [38] L.V. Shilei, F. Guohui, Z. Neng and D. Li, Experimental study and evaluation of latent heat storage in phase change materials wallboards, *Energy and buildings* 39 (2007) 1088-1091.
- [39] X. Wang, Z. Shen, Y. Zhang and D. Li, Mechanical and thermal properties of PCM wallboards based on gypsum and paraffin, *Applied Mechanics and Materials*, 71-78 (2011) 3553-3557.
- [40] J.J. Tomlinson and D.D. Heberle, Analysis of wallboard containing a phase change material, *Proceedings of the 25th Annual Intersociety Energy Conversion, Engineering Conference*, Reno, NV (1990).
- [41] Z.X. Gong and A.S. Mujumdar, Enhancement of energy charge-discharge rates in composite slabs of different phase change materials, *Int. J. Heat and Mass Transfer*, 39 (4) (1996) 725-733.
- [42] S. Shaikh and K. Lafdi, Effect of multiple phase change materials (PCMs) slab configurations on thermal energy storage, *Energy Conversion and Management* 47 (2006) 2103-2117.
- [43] The Weather Channel, www.weather.com
- [44] The Weather Underground Inc, www.wunderground.com
- [45] Y. Lee, M.S. Choi, S.T. Yi and J.K. Kim, Experimental study on the convective heat transfer coefficient of early-age concrete, *Cement and Concrete Composites* 31(1) (2009) 60-71
- [46] B. Gibbs and S. Hasnain, DSC study of technical grade phase change heat storage materials for solar heating applications, In: *Proceedings of the 1995 ASME/JSME/JSEJ International Solar Energy Conference, Part 2* (1995).
- [47] A. Sharma, V. V. Tyagi, C. R. Chen and D. Buddhi, Review on thermal energy storage with phase change materials and applications, *Renewable and sustainable energy reviews* 13 (2009) 318-345.
- [48] BASF Corporation, The Chemical Company, www.basf.com
- [49] Rubitherm Technologies GmbH, www.rubitherm.de/english/index.htm
- [50] Entropy Solutions, Inc., <http://www.puretemp.com/>
- [51] Solar Panels Plus LLC, www.solarpanelsplus.com/ (accessed on June 2011)

[52] National Renewable Energy Laboratory (NREL) - http://rredc.nrel.gov/solar/old_data/nsrdb/1961-1990/redbook/sum2/state.html (accessed on June 2011)

[53] H. E. Feustel and C. Stetiu, Thermal Performance of Phase Change Wallboard for Residential Cooling Application, Lawrence Berkeley National Laboratory, Berkeley, CA (1997).

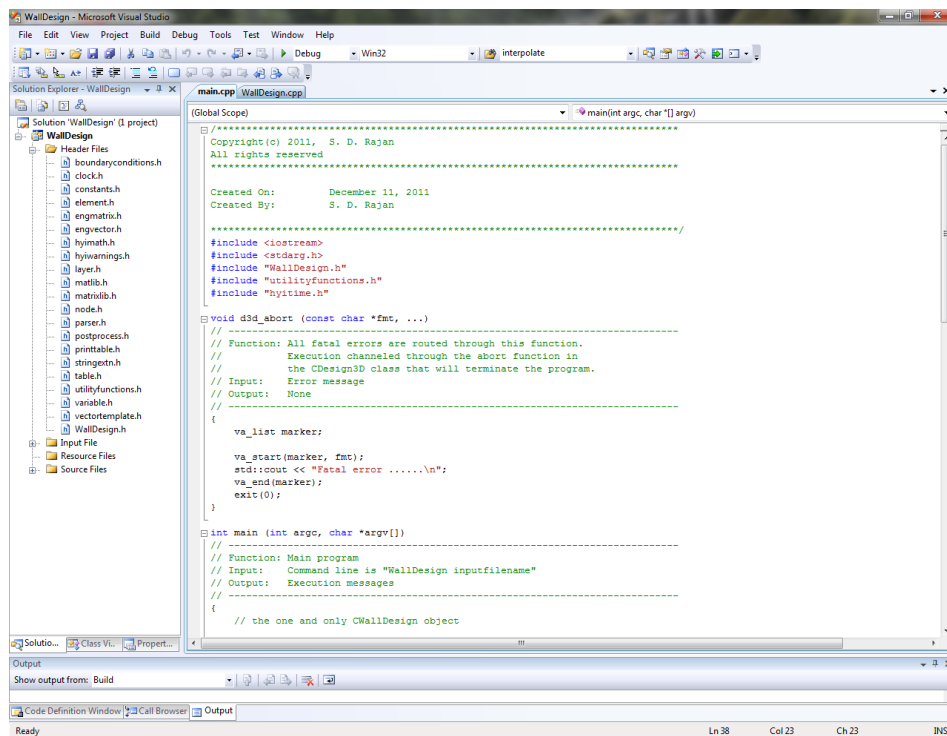
[54] K. Roth, D. Westphalen, J. Dieckman, S. Hamilton and W. Goetzler, Energy Consumption Characteristics of Commercial Building HVAC Systems Volume III, Building Technologies Program (2002) A-108.

APPENDIX

WALL DESIGN PROGRAM

Introduction

The wall design program is used to carry out linear or non-linear two-dimensional transient heat transfer analysis on any homogeneous or composite rectangular structure, along with optimization of the material thicknesses of the structure. The program is specifically made using Microsoft Visual Studio C++ (2010) dependent on ABAQUS V6.9-1. It cannot be run without the aid of ABAQUS or the ABAQUS output files. Only structures with uniform cross-section in the z-direction can be analyzed, since the program considers only 2D surfaces. Heat is assumed to flow only in the x-direction (unidirectional). Any irregularities in the geometry of the model are ignored.



```
main.cpp [WallDesign.cpp]
(Global Scope)
main(int argc, char *[] argv)
.....
Copyright (c) 2011, S. D. Rajan
All rights reserved
.....
Created On: December 11, 2011
Created By: S. D. Rajan
.....
.....
#include <iostream>
#include <string>
#include "WallDesign.h"
#include "utilityfunctions.h"
#include "hysitime.h"
.....
void d3d_abort(const char *fmt, ...)
// Function: All fatal errors are routed through this function.
// Execution channeled through the abort function in
// the CDesign3D class that will terminate the program.
// Input: Error message
// Output: None
//
{
    va_list marker;
    va_start(marker, fmt);
    std::cout << "Fatal error ..... \n";
    va_end(marker);
    exit(0);
}

int main(int argc, char *argv[])
// Function: Main program
// Input: Command line is "WallDesign inputfilename"
// Output: Execution messages
//
{
    // the one and only CWallDesign object
}
```

Figure 6-1: WallDesign Program

Program Execution

Input file name has to be specified as an essential command argument. Use the process below to enter the filename in the format mentioned. There are three options of the type of analysis that can be executed that include FE analysis, post process only and optimization. The FE analysis creates an ABAQUS model and then analyzes outputs the results of the given model. This is performed by using the “-fea” command in the command arguments. The post process only runs just the computational part of the energy analysis after the ABAQUS output file (*.dat) is already present. This is done by using the “-postprocess” command in the command arguments. The optimization of the model can be performed using the “-optimize” command.

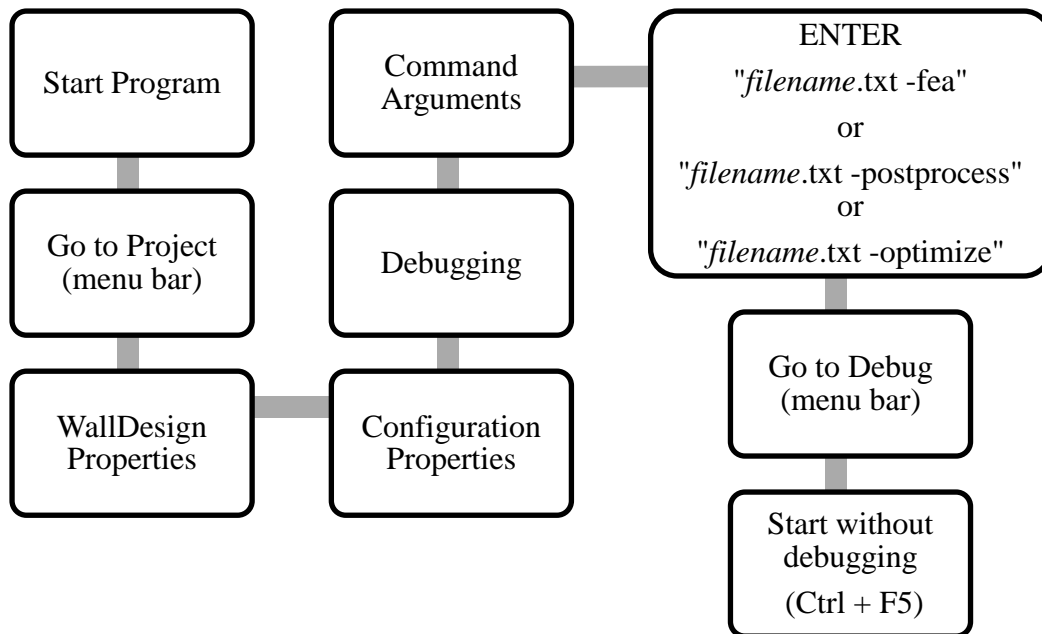


Figure 6-2: Procedure to start program

Algorithm

1. Check number of input arguments and process accordingly
2. Check total number of runs and loop through each run separately
3. Open I/P and O/P files
4. Read data from Input ("*.txt") file
5. Write ABAQUS input file ("*.inp")
6. Launch ABAQUS and analyze the input file
7. ABAQUS creates the output file ("*.dat") from the heat analysis
8. Read data from ABAQUS output file ("*.dat")
9. Start POST PROCESSING ABAQUS results
10. Loop through all time steps
11. Calculate the value of Energy flow through inside face (EFTIF) and
Energy flow through outside face (EFTOF)
12. Loop through all elements
13. Calculate values for Latent energy, Sensible energy and Total energy
stored in each element and sum them up for each time step
14. Print all values of energy to the output file
15. Optimize if appropriate (see the optimization section later)
16. Close all files and terminate program

Program Organization

OutputBanner :

This function prints a banner with license, time and date of analysis on each output file.

FEAOnly :

This function runs all appropriate functions for carrying out the FE analysis and re-runs entire analysis for number of specified run times.

PostProcessOnly :

This function runs all appropriate functions for performing the post process analysis only and re-runs entire analysis for number of specified run times.

Optimize :

Runs all appropriate functions for carrying out the optimization process

Interpolate :

Function to interpolate between any given set of x-y values, when called.

VerifyCommandLineInput :

The function adds the non-optional input file name along with either “-fea”, “-postprocess” or “-optimize” arguments to the program. The “-fea” lets FE analysis in ABAQUS take place. The “-postprocess” option lets you skip the ABAQUS analysis and carry out only post-processing. The “-optimize” lets

optimization of the model to take place. Function also creates and opens the input file.

OpenOutputFiles :

Opens the ABAQUS input file (if needed) and all the output files.

TerminateProgram and CloseAllFiles :

Closes all files and exits the program.

ReadInputFile :

Reads the input (“*.txt”) file and stores all data required. The function runs through the input file twice, the first time to set all the variable sizes and get a rough estimate of the number of parameters. During the second pass all the data is stored in the required structure.

Analyze :

According to the size of the elements given or the number of elements through thickness given in the input file, a mesh is generated (i.e. nodal and elemental data for the FE analysis in ABAQUS are generated) and the data is printed to the ABAQUS input file (“*.inp”). Also, the input file is completed with all time steps, material data and boundary conditions. After completion of the input file the ABAQUS command program is launched and the input file is processed to create the FE model and ABAQUS output file to use for post processing.

PostProcess :

After ABAQUS analysis is complete, the function reads the nodal temperature and elemental heat flux data from the ABAQUS output file ("*.out") and stores it in an appropriate structure.

ComputeStoredEnergy_Version2:

This function carries out all the post-processing procedures mentioned in the next section.

ErrorHandler :

The error handler function detects any errors in the input file, analysis or the post-processes and exits the program with the appropriate error message.

POST PROCESSING

After the ABAQUS analysis is complete and the ABAQUS output file gives the data for nodal temperature and heat flux at every point for all time steps, the Wall Design program stores and processes this data and creates another set of energy related outputs. The program runs a nested loop for each time step and each element. Energy stored in the form of sensible heat, latent heat and the total energy stored are calculated separately for each element, and then summed over all elements for each time step. Output from the program gives cumulative sensible energy, cumulative latent energy and step-wise total energy stored in each layer during each time step. From the output data, the maximum value of the latent energy stored in PCM is used to compute efficiency.

Energy flow through the inside and outside walls is calculated using the heat flux data from the ABAQUS output file. For each set of either outer or inner elements, the flux obtained is multiplied by the (outer or inner) surface area to obtain energy flow through each surface for every time step. If the flux is negative (i.e. heat flows into the wall on the inside and out of the wall on the outside) energy flow is also considered to be negative. The positive and negative energy flow through the (outer and inner) face of the wall is tabulated separately in the output file for every time step, summation of which gives us the total energy flow.

OUTPUT FILES

The program WallDesign creates 5 different output files. If the Debug Level of the program is set to 0, only the first two output files are generated. If the debug level is set to 1, all the output files are generated.

1) filename_Output.out

This is a text file which stores Energy flow through outer and inner face and the energy stored by each layer for every time step. It also outputs the energy storage capacity of the PCM in a single line at the bottom.

2) filename_OutputALL.xls

This is an excel format output file that stores the below data only for the output increments desired.

Time Step, Sensible heat stored, Latent heat stored, Energy flow through Inner face (EFTIF), PCM Efficiency (PCME), Outer face temperature, interface temperature's for all layers, inside face temperature,

temperature of nodes just before the inside face, Left end applied temperature., Right end applied temperature.

3) filename_NT.xls

This is an excel (2003-2007) format output file that stores the Nodal temperature data for the outer, inner and interface nodes for all time steps.

4) filename_OutputEnergy.xls

This is an excel (2003-2007) format output file which stores the cumulative values of sensible energy, latent energy, total energy stored in the PCM respectively.

5) filename_Output1.xls

This is an excel (2003-2007) format output file that stores the following data, for each element for each time step. Values output are only for the particular element.

Time Step, Layer No., Element #, Initial Temp, final Temp, Delta T, Sensible heat stored, Latent heat stored, Total energy stored (cumulative), specific heat capacity, Latent heat per degree, mass of element.

INPUT FILE FORMAT

*heading

Analysis of concrete wall

*units

length, m

mass, kg

time, s

temperature, K

energy, J

*parameter

**name, value

H, 1.0

(Height of model)

T_CONCRETE, 5

(thickness of Layer 1)

T_PCM, 5

(thickness of Layer 2 and so on)

E_CONCRETE, 2

(# of elements through thickness desired for Layer 1)

E_PCM, 2

(# of elements through thickness desired for Layer 2 and so on)

*sel, value

Constant value of element thickness (to be used instead of value of # of elements through thickness)

*debug level, 0 or 1

Value of 0 or 1 will decide which output files are to be printed

*run, 1, Name1

of sets of different BC's to be applied and name of file to be printed

*dimensions

**Height x Thickness

H, T_CONCRETE+T_PCM

Parameters used for denoting height and total thickness of model

*table, name1, # of rows, # of columns,
Time

Time to be mentioned only if x-data is time

x1, y1

x2, y2
x3, y3 and so on
**table, name2, # of rows, # of columns, Repeat for as many tables as required*
Time
x1, y1
x2, y2
x3, y3 and so on
**layer Define layer name, geometry and material properties*

***name, thickness, number of elements through thickness*
Concrete, T_Concrete, E_Concrete
***density, conductivity or table name, specific heat or table name*
2400.0, 1.45, 750.00
***latent, solidus temperature, Liquidus (replace with 0 if no value is to be assigned), temperature Repeat layer data for all layers*

0, 0, 0
**initial temperature Initial condition of model*
1, value Run # and initial temperature

**time steps*
***# of time steps, final time value, output increment start, output increment end*
48, 172800, 25, 48 Final time value should be in consistent units. Output will be displayed on for the increments mentioned

**left end bc*
***Run #, type, table name, value 1, value 2*

** 1, mixed, Table1, 1.0, 20.0 If BC type is mixed, and temperature varies over time. Value 1 is the base value for which amplitude is specified, Value 2 is heat transfer co-efficient for left end*

** 1, mixed, , 300.0, 20.0 If BC type is mixed, and temperature remains constant over time. Value 1 is the temperature, Value 2 is heat transfer co-efficient for left end*

SAMPLE INPUT FILE

Model Details:

Input file has been written for a 20cm thick concrete wall (1m in height) with a 1cm PCM layer placed at the center of the wall. Ambient air temperature acts on the outside face, i.e. mixed BC over 24 hours. 2 different sets of ambient temperature and inside temperature have been applied to the wall for 2 separate days. Conductivity and specific heat capacity of the PCM vary with temperature. Mixed BC of 300 K acts on the inside face (i.e. temperature of the air inside is constant at 300 K). Initial temperature of the wall for day 1 is 296 K and day 2 is 280 K. Outside and inside heat transfer coefficients are 20 and 5 W/m²-K respectively. Output is desired only from 20-24 hours. Element size is fixed at 0.5cm.

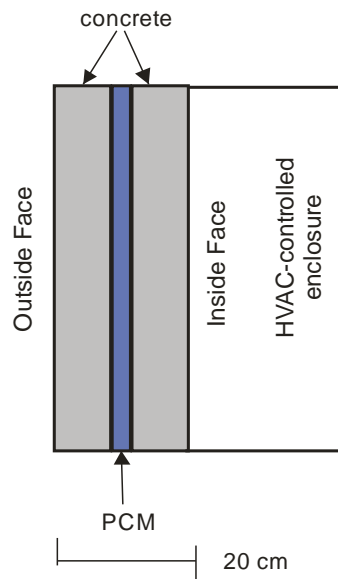


Figure 6-3: Model details for sample input file

INPUT FILE

*heading

Analysis of a 20cm Wall - 1cm PCM placed in center of wall

*units

Length, m

Mass, kg

Time, s

Temperature, K

Energy, J

*parameter

**name, value

H, 1.0

T_CONCRETE1, 0.095

T_PCM, 0.01

T_CONCRETE2, 0.095

E_CONCRETE1, 2

E_PCM, 2

E_CONCRETE2, 2

*sel, 0.005

*debug level, 0

*run, 2, Day1, Day2

*dimensions

**Height x thickness

H, T_CONCRETE1+T_PCM+T_CONCRETE2

*table, CONDPCM, 4, 2

0.2206 , 273 ,

0.2233 , 284 ,

0.214 , 288 ,

0.1838 , 309 ,

*table, SHPCM, 4, 2

3670 , 275 ,

5400 , 287 ,

15000 , 295 ,

4200 , 305 ,

*table, CONV1, 24, 2, TIME

3600 , 299.3775

7200 , 301.1996

10800 , 303.0223

14400 , 304.6773

18000 , 305.7222

21600 , 306.4888

25200 , 306.6441

28800 ,	306.3554
32400 ,	305.4553
36000 ,	304.2772
39600 ,	302.7111
43200 ,	300.9779
46800 ,	299.0771
50400 ,	297.2337
54000 ,	295.3892
57600 ,	293.5441
61200 ,	292.0335
64800 ,	290.6887
68400 ,	289.73366
72000 ,	289.27805
75600 ,	289.26634
79200 ,	290.1446
82800 ,	291.9109
86400 ,	294.567

*table, CONV2, 24, 2, TIME

3600 ,	281.3
7200 ,	282.4
10800 ,	284.1
14400 ,	284.6

18000 ,	285.7
21600 ,	286.3
25200 ,	286.3
28800 ,	286.3
32400 ,	285.7
36000 ,	283.5
39600 ,	282.4
43200 ,	282.4
46800 ,	281.3
50400 ,	280.7
54000 ,	280.2
57600 ,	277.4
61200 ,	277.4
64800 ,	278
68400 ,	278
72000 ,	276.8
75600 ,	276.8
79200 ,	276.8
82800 ,	278.5
86400 ,	279.1

*layer, 1

**name, thickness, number of elements through thickness

CONCRETE1, T_CONCRETE1, E_CONCRETE1

**density, conductivity or table name, specific heat or table name

2400.0, 1.45, 750.0

**latent heat, solidus temp, Liquidus temp

0, 0, 0

*layer, 2

**name, thickness, number of elements through thickness

PCM, T_PCM, E_PCM

**density, conductivity or table name, specific heat or table name

1000, CONDPCM, SHPCM

**latent heat, solidus temp, Liquidus temp

194000, 298, 302

*layer, 3

**name, thickness, number of elements through thickness

CONCRETE2, T_CONCRETE2, E_CONCRETE2

**density, conductivity or table name, specific heat or table name

2400.0, 1.45, 750.0

**latent heat, solidus temp, Liquidus temp

0, 0, 0

*initial temperature

1, 296.0

2, 280.0

*time steps

**# of time steps, final time value, output increment start, output increment end

24, 86400, 20, 24

*left end BC

** Run #, type, table name, value 1, value 2

1, mixed, CONV1, 1.0, 20.0

2, mixed, CONV2, 1.0, 20.0

*right end BC

** Run #, type, table name, value 1, value 2

1, mixed, 300.0, 1.0, 5.0

2, ebc, 290.0

*postprocess

stored_energy, PCM

energy_flow, rightend

*end